Dll1 and Jag1 are Differentially Required to Specify

Proximal and Distal Pancreatic Duct Compartments

Philip A. Seymour[1], Caitlin A. Collin[1], Mette C. Jørgensen[1], Itaru Imayoshi[2],

Ryoichiro Kageyama[2] and Palle Serup[1*]

[1] The Danish Stem Cell Center (DanStem), Faculty of Health Sciences, University of Copenhagen,

Blegdamsvej 3B, Copenhagen N, DK-2200, Denmark

[2]Institute for Virus Research, Kyoto University, Kyoto 606-8507, Japan

* Corresponding Author:

E-mail: palle.serup@sund.ku.dk

Telephone: +45 40 22 00 26

Fax:

Abstract

Pancreatic β-cells arise from bipotent trunk progenitors (TrPCs) that are specified from multipotent pancreatic progenitors (MPCs) in a Notch-dependent manner. The time window during which Notch signaling is required to specify TrPCs and the identity of the Notch ligands required for this patterning process remain obscure. Here we show that blocking Notch signal transduction before E13 drives progenitors to an acinar fate while blockade after E13 results in amplified and accelerated endocrine differentiation. Mapping of Dll1 and Jag1 expression using IF and novel targeted reporters revealed that uniform Jag1 expression in E10.5 MPCs becomes restricted to distal Ptf1a$^+$ tip progenitors (TiPCs) during PD patterning. Conversely, Dll1 is expressed in scattered MPCs, TrPCs, and TiPCs, and in Neurog3$^+$ endocrine precursors at all stages. Endodermal deletion of *Jag1* delays resolution of tip and trunk domains, and at E15.5 distal Sox9$^+$ TrPCs are replaced by Ptf1a$^+$ Mist1$^+$ cells. Remarkably, this occurred with negligible impact on pancreas size and gross morphology of the ductal tree despite the replacement of TrPCs with TiPCs in the duct-lining epithelium. Some Sox9$^+$ progenitors remain proximally in the prospective main duct and loss of β-cells is not complete. However, endodermal deletion of *Dll1* and *Jag1* ablated the remaining Sox9$^+$ TrPCs and β-cells entirely at E15.5, while normal specification of Sox9$^+$ TrPCs was seen in *Dll1* single mutants. Together, our results reveal a shift in competence of *Hnf1β*$^+$ progenitors around E13 and show that multiple cellular sources provide Notch ligand input to specify different parts of the pancreatic epithelium prior to E13.

Introduction

The signaling milieu in the pancreatic progenitor niche is highly dynamic such that a given cue can exert disparate, even opposing effects at distinct stages and in different cell populations contingent upon cellular context. As an exemplar, the Notch signaling pathway not only inhibits but also promotes differentiation of insulin$^+$ β-cells during different stages of the pancreatic program. Defining temporal window(s) of Notch-dependent processes in β-cell formation as well as the source of Notch ligands is important to understand the β-cell differentiation program and inform the rational design of *in vitro* β-cell differentiation protocols.

The mammalian pancreas arises as dorsal and ventral evaginations of the posterior foregut endoderm, becoming discernible in the mouse at around embryonic day (E)8.75-9.0 (Wessells and Cohen, 1967), lagging several hours behind pancreatic fate specification evidenced by onset of *Pdx1* expression (Offield et al., 1996; Ohlsson et al., 1993). From outgrowth on, until around E12 when the paired buds are rapidly expanding and branching, the pancreatic epithelium largely comprises multipotent pancreatic progenitor cells (MPCs), distinguished by their expression of several transcription factors including Pdx1, Ptf1a, Hnf1β, Sox9 and Nkx6.1. MPCs give rise to both the exocrine pancreas - the digestive enzyme-producing acinar cells and the ductal cells which transport them to the intestine - and the endocrine islet cells, of which insulin$^+$ β-cells comprise the majority (Gu et al., 2002; Kopinke et al., 2011; Kopp et al., 2011; Pan et al., 2013; Solar et al., 2009; Zhou et al., 2007). Endocrine differentiation proceeds through a transient endocrine precursor expressing high levels of the transcription factor Neurogenin3 (Ngn3), which is both necessary and sufficient for endocrine differentiation (Apelqvist et al., 1999; Gradwohl et al., 2000; Grapin-Botton et al., 2001). By E12.5 the paired buds fuse and a ductal tubular plexus is established. Over the next week a synchronous extension and reorganization of the tubular plexus remodels this domain into a unified ductal tree (Kesavan et al., 2009; Villasenor et al., 2010). Concurrent with this remodeling of the epithelium, the process of proximodistal (PD) patterning which occurs between ~E10.5 to ~E14.5 resolves Ptf1a$^+$ Nkx6.1$^+$ MPCs into two developmentally and spatially segregated populations: distally-localized unipotent Ptf1a$^+$ Nkx6.1$^-$ "tip" progenitors (TiPCs) committed to an acinar fate and proximal Ptf1a$^-$ Nkx6.1$^+$ "trunk" progenitors (TrPCs) which are endocrine-/duct-bipotent: TrPCs attaining an Ngn3^{Hi} state initiate an endocrine program and delaminate from the polarized epithelium with those progenitors failing to do so remaining *in situ* and adopting a ductal

fate (Hald et al., 2008; Schaffer et al., 2010; Zhou et al., 2007). Genetic mouse models have revealed PD patterning to be driven by a cross-repressive antagonistic loop between Ptf1a and Nkx6.1/Nkx6.2 (Nkx6) with forced Ptf1a expression promoting TiPC commitment while forced Nkx6 expression supports adoption of TrPC fate (Schaffer et al., 2010). A role for Notch signaling in this process was first implicated by the finding that clonal analysis of cells with forced expression of Notch1 intracellular domain (N1ICD) showed them to segregate to an Nkx6.1^{+} fate (Schaffer et al., 2010).

Notch receptors are activated at the plasma membrane by DSL (Delta, Serrate, Lag-2) transmembrane ligands expressed by adjacent cells, comprising members of the Delta-like (Dll) and Jagged families in mammals, initiating ADAM-then γ-secretase-mediated cleavage events, which liberate the Notch intracellular domain (NICD), allowing it to translocate to the nucleus. There, NICD functions as a transcriptional activator by binding to Rbp-jk and recruiting the cofactor Mastermind-like (Maml) and, replacing co-repressors with co-activators to activate the transcription of Notch downstream targets, most notably *Hes1* (Bray, 2016). In the context of pancreas morphogenesis, Notch signaling and *Hes1* are required for maintaining the proliferation and undifferentiated status of MPCs by preventing precocious and excessive endocrine differentiation (Ahnfelt-Rønne et al., 2012; Apelqvist et al., 1999; Jensen et al., 2000). More recently, it was discovered that active Notch signaling is required to commit MPCs to the duct/endocrine-competent TrPC fate: in addition to forced N1ICD expression being shown to promote TrPC commitment (Schaffer et al., 2010), additional genetic mouse models of Notch signaling blockade (forced expression of dominant-negative - dn - Maml1 or conditional deletion of *Mib1* or *Hes1*) resulted in a gain of TiPCs at the expense of a loss of the TrPC population (Afelik et al., 2012; Horn et al., 2012). This TrPC-promoting effect of Notch signaling has been speculated to be achieved *via* direct upregulation of Nkx6.1 expression since Rbpj binds the *Nkx6.1* promoter during PD patterning (Afelik et al., 2012). Once specified, Notch signaling and Hes1 expression persist in TrPCs where they serve to maintain Sox9 expression and ductal fate, and to inhibit endocrine differentiation by repressing *Ngn3* (Bankaitis et al., 2015; Klinck et al., 2011; Kopinke et al., 2011; Magenheim et al., 2011; Shih et al., 2012). Collectively, these studies show that Notch signaling is required iteratively during the pancreatic program, first to maintain MPCs, then to actively allocate them to a duct/endocrine-competent TrPC fate and subsequently to maintain ductal identify by repressing an endocrine program. However, a number of questions remain unresolved. Foremost amongst these are: 1) what is the temporal

window through which Notch signaling is required to allocate MPCs to a TrPC fate, 2) which cells are signal-sending (so, ligand-expressing) and -receiving cells during PD patterning and beyond, and 3) which ligands are expressed during the various stages of pancreas morphogenesis and which are involved in regulating various cell fate decisions? In mice, the DSL ligand family, comprises Jag1, Jag2, Dll1, and Dll4, while the atypical Delta-type ligand Dll3 is thought to act as an intracellular inhibitor of Notch signaling (Chapman et al., 2011; Geffers et al., 2007; Ladi et al., 2005). Which of the four trans-activating Notch ligands that orchestrate receptor activation at different stages and in different cell fate decisions during pancreatic development remains ill-defined. This is in part a consequence of the lack of validation of commercially-available antibodies and the perdurance of transcriptionally-uncoupled reporters in existing ligand reporter lines. This inability to accurately report real-time expression of Notch ligands is especially problematic given the inherently dynamic nature of Notch signaling (Shimojo and Kageyama, 2016).

In the present study, we elected to focus upon interrogating the role of Notch signaling in governing a single fate decision during the pancreatic program, namely allocation of MPCs between the TiPC and TrPC lineages during PD patterning, given the crucial requirement for the latter in generating duct and endocrine cells. Here we show that blockade of Notch signal reception by expression of a dnMaml1-eGFP fusion protein in *Sox9*$^{+}$ *Hnf1β*$^{+}$ cells prior to ~E13 diverts these into a Ptf1a^{+} acinar fate. Blocking Notch reception at later stages results in induction of accelerated endocrine differentiation revealing closure of the window of Notch-dependent TrPC specification at ~E13. Through spatiotemporal expression analysis of both novel Venus fusion protein *Jag1* and *Dll1* reporters and endogenous ligands using validated antibodies, we identified Jag1 and/or Dll1 as strong candidates for the TrPC-specifying signal. Novelly, we show Jag1 expression to be specific to the distal TiPC domain during PD patterning with Dll1 expressed in both proximal Ngn3^{+} endocrine precursors and Ngn3^{-} MPCs. By inactivating ligand trans-activating function *via* deletion of *Mib1* in *Ptf1a*$^{+}$ TiPC-fated progenitors, we functionally show that TiPC-derived Notch signals are required for specifying the distal-most (TrPC-derived) duct/centroacinar cells. Finally, by examining single or conditional compound mutant mice deficient for endodermal *Jag1* and/or *Dll1*, we show that TiPC-derived *Jag1* is responsible for specifying ~90% of the TrPC population with the remaining proximal-most TrPCs being specified by more proximal Dll1-mediated cues. Taken together, our data suggest

that multiple cellular sources of Notch ligands are required to properly commit MPCs to the duct/endocrine-competent TrPC fate prior to E13.

Results and Discussion

Notch Signaling Transduction is Required to Allocate MPCs to a TrPC Fate

In order to define the temporal window through which active Notch signaling is required to commit MPCs in the early pancreas to the TrPC fate, the ability to receive and/or transduce Notch signals was abrogated in TrPC-biased MPCs and their progeny. This was achieved *via* stable and heritable expression of a *Rosa26* (*R26*) locus-targeted dnMaml1-eGFP fusion protein (Horn et al., 2012) in TrPC-fated progenitors and their descendants using TrPC-specific *Hnf1β*-CreER^{T2} (Solar et al., 2009) during PD patterning. The *R26*$^{dnMaml1\text{-}eGFP}$ fusion protein has been shown to be a potent and specific inhibitor of all four mammalian Notch receptors *in vivo* (High et al., 2008; High et al., 2007; Maillard et al., 2008; Maillard et al., 2004; Tu et al., 2005). Notch reception was abrogated in TrPC-fated progenitors from E12, conjectured to fall during the window of active PD patterning on the basis of: 1) co-expression of Nkx6.1 and Ptf1a in MPCs largely resolving into distinct trunk and tip domains respectively between E10.5 and E14.5 (Schaffer et al., 2010) and 2) lineage-tracing showing the potency of *Ptf1a*$^{+}$ cells and *Hnf1β*$^{+}$ cells narrowing from being multipotent at E11 to principally acinar- (*Ptf1a*$^{+}$) or duct/endocrine- (*Hnf1β*$^{+}$) committed by E14 (Pan et al., 2013; Solar et al., 2009). To accomplish this, a single dose of tamoxifen was administered intraperitoneally at E11.5 to pregnant dams carrying compound-heterozygous *Hnf1β-CreER*^{T2}*; R26*$^{dnMaml1\text{-}eGFP}$ embryos. Following tamoxifen exposure, *Hnf1β*-CreER^{T2}-mediated recombination of the *R26*$^{dnMaml1\text{-}eGFP}$ allele renders *Hnf1β*$^{+}$ TrPC-biased MPCs and their progeny incapable of receiving and/or transducing Notch signals. Expression of the dnMaml1-eGFP fusion protein not only inhibits all Notch receptors but also indelibly and heritably labels such "Notch-deaf" cells and their descendants with eGFP, allowing their cell fate within the pancreas to be assessed (**Fig. 1A**). Double-heterozygous embryos carrying *Hnf1β-CreER*^{T2} and the *R26*^{YFP} Cre reporter allele (Srinivas et al., 2001) with tamoxifen administered in an identical manner served as controls, allowing *Hnf1β-CreER*^{T2}-recombined Notch signaling-intact cells to be YFP-labeled for lineage-tracing (**Fig. 1B**). This approach enables relative tissue contributions of Notch-deaf and control Notch-intact TrPCs and their progeny to be directly compared by controlling for differing mitotic indices of the various cell types given that dnMaml1

expression has previously been shown not to affect proliferation rates of pancreatic progenitors (Afelik et al., 2012). Relative tissue contributions of lineage-labeled cells were assessed at the mid-point of the secondary transition (E15.5) by co-immunofluorescence (IF) analysis on serial sections for GFP (antisera detect both eGFP and YFP). We used two different combinations of lineage markers, either: 1) Ptf1a (TiPC-derived acini) and Sox9 (TrPC-derived endocrine/duct-competent bipotent progenitors) or 2) Sox9, Ngn3 (endocrine precursors) and chromogranin-A (endocrine cells) (**Fig. 1D**). Availability of discriminable fluorescent conjugates and antibody host species precluded simultaneous detection of the five markers. Thus, similar proportions of lineage-labeled cells should prove Sox9$^+$ on adjacent sections using the two antisera combinations. Likewise, the proportion of traced cells scoring as Sox9$^-$ Ptf1a$^-$ in combination 1 should be similar to those expressing Ngn3 or chromogranin-A on the adjacent section receiving combination 2, given that Sox9$^-$ Ptf1a$^-$ pancreatic trunk epithelial cells are highly likely to be endocrine cells or their immediate Ngn3$^+$ precursors. The close concordance of these parameters between the two antisera combinations illustrates the robustness and internal consistency of the analyses.

Initial analyses of E12.5 pancreata from *Hnf1β-CreER^{T2}* embryos carrying either *R26^{YFP}* (control) or *R26$^{dnMaml1\text{-}eGFP}$* (mutant) alleles exposed to a single pulse of tamoxifen 24 hours earlier at E11.5 revealed YFP or eGFP labeling respectively in only a small fraction of Hnf1β$^+$ MPCs (data not shown). Embryonic lethality precluded injecting higher doses of tamoxifen than the 75 µg/g regimen employed throughout these analyses. The low recombination efficiency of *Hnf1β*-CreER^{T2}, which is consistent with the initial characterization of this strain (Solar et al., 2009), produced near single-cell mosaic clonal labeling within the dorsal and ventral pancreatic epithelium. No YFP or dnMaml1-eGFP labeling was detectable in the absence of *Hnf1β-CreER^{T2}*, in any embryos examined (data not shown).

Examination of pancreata at E15.5 following tamoxifen injection at E11.5 revealed that in *Hnf1β-CreER^{T2}; R26^{YFP}* control pancreata, over three-quarters of Notch-intact YFP$^+$ cells expressed markers of TrPC-derived cells: Sox9$^+$ bipotent progenitors (~40% of YFP$^+$ cells were Sox9-immunopositive), endocrine precursors (14.0% of YFP$^+$ cells were Ngn3$^+$) and endocrine cells (31.2% of YFP$^+$ cells were chromogranin-A$^+$) (**Fig. 1E,G,H,J**). In contrast, only 24.7% of YFP$^+$ cells co-expressed the TiPC and acinar cell marker Ptf1a (**Fig. 1E,G**). This contribution of *Hnf1β-CreER^{T2}*-labeled progenitors to all three main lineages (but ostensibly biased towards TrPC-derived duct and

endocrine cells notwithstanding different cell type-specific proliferation rates) following tamoxifen injection at E11.5 is in close accordance with primary lineage-tracing analyses using the *Hnf1β-CreER*^{T2} line (Solar et al., 2009). As CreER undergoes translocation to the nucleus ~6-12 hours post tamoxifen-injection and remains there for approximately 36 hours following administration (Ahn and Joyner, 2004; Danielian et al., 1998), these findings show that at the population level, *Hnf1β*$^{+}$ cells are multipotent through the E12-E13 pulse-labeling window resulting from an E11.5 tamoxifen injection (**Fig. 1C**).

In stark contrast to control pancreata, when examined at E15.5 following E11.5 tamoxifen injection, significantly fewer - less than 4% - of dnMaml1-eGFP^{+} Notch-abrogated cells in *Hnf1β-CreER*^{T2}*; R26*$^{dnMaml1\text{-}eGFP}$ pancreata co-expressed Sox9, consistent with previous work (Afelik et al., 2012)(**Fig. 1F,G,I,J**). Thus, rendering a progenitor incapable of receiving Notch signals disallows its allocation to the TrPC-derived bipotent progenitor/duct fate. Instead, more than two-thirds of dnMaml1^{+} Notch-deaf cells expressed markers consistent with a Ptf1a^{+} (or Sox9^{-} Ngn3^{-} chromogranin-A^{-}) acinar identity (**Fig. 1F,G,I,J**)). This is concordant with blockade of Notch signaling preventing MPCs from committing to a TrPC fate, re-allocating TrPC-destined progenitors to the alternative Notch-independent TiPC lineage (Afelik et al., 2012; Horn et al., 2012). In addition to the acinar lineage, Notch-abrogated progenitors also contributed to the endocrine lineage with a similar propensity as Notch-intact progenitors in control pancreata: 22.2% of dnMaml1-eGFP^{+} cells co-expressed either chromogranin-A or Ngn3, using antibody combination 2, while 26.5% were Sox9^{-} Ptf1a^{-} using antibody combination 1 (**Fig. 1E-J**). Thus, dnMaml1-mediated inhibition of Notch reception does not induce precocious endocrine differentiation, consistent with previous work (Afelik et al., 2012). Notably, significantly fewer dnMaml1-eGFP^{+} cells co-expressed Ngn3 (0.4%) compared with the YFP-labeled cells in control *Hnf1β-CreER*^{T2}*; R26*^{YFP} pancreata (14.0%) (**Fig. 1H-J**). Thus, at E15.5, approximately three days following abrogation of Notch reception, *Hnf1β*$^{+}$ progenitors and their progeny are approximately 35-fold less likely to embark on an endocrine program compared with Notch-intact progenitors in control pancreata. This could suggest that sustained dnMaml1 expression in TrPCs and their progeny impedes *Ngn3* activation or alternatively, that many Ngn3^{+} cells are not fully committed to an endocrine fate and are diverted to a Ptf1a^{+} acinar fate. A precedent for this notion exists in that *Ngn3*-Cre-mediated deletion of Presenilins 1

and 2 appears to divert *Ngn3*$^+$ cells to an acinar fate (Cras-Meneur et al., 2009). A lowering of *Ngn3* gene dosage has the same effect (Wang et al., 2010).

The Window of Notch-Dependent TrPC Allocation Closes by E13

Having confirmed that active Notch signaling is required to allocate MPCs to a TrPC fate at E12-E13, we sought to define the temporal window through which TrPC commitment is Notch-dependent. To this end, cellular contributions of Notch-deaf *versus* Notch-intact TrPCs and their progeny were assessed in E15.5 *Hnf1β-CreER*^{T2}*; R26*$^{dnMaml1\text{-}eGFP}$ and *Hnf1β-CreER*^{T2}*; R26*^{YFP} pancreata following tamoxifen injection at either E12.5 or E13.5 (**Fig. 1C**). Following E12.5 tamoxifen injection, approximately a third of Notch-intact YFP$^+$ cells in *Hnf1β-CreER*^{T2}*; R26*^{YFP} control pancreata expressed Sox9 while around half expressed endocrine markers (13.0% of YFP$^+$ cells were Ngn3$^+$, 41.0% were chromogranin-A$^+$, using antibody combination 2; and 48.8% were Sox9$^-$ Ptf1a$^-$ using antibody combination 1); fewer than 20% co-expressed acinar markers (18.1% were Ptf1a$^+$; 13.5% were Sox9$^-$ Ngn3$^-$ chromogranin-A$^-$)(**Fig. 1K,M,N,P**). Tamoxifen injection at E13.5 revealed an even more pronounced distribution of control Notch-intact YFP-labeled progenitors towards TrPC derivatives: 45% of YFP$^+$ cells were Sox9$^+$ and a further 41.1% expressed endocrine markers (22.5% of YFP$^+$ cells expressed chromogranin-A while 18.6% were Ngn3$^+$); only 6.8% of YFP$^+$ cells were Ptf1a$^+$ (13.4% were Sox9$^-$ Ngn3$^-$ chromogranin-A$^-$)(**Fig. 1Q,S,T,V**). Thus, while *Hnf1β*$^+$ cells retain their multipotency at E13 and E14 (E12.5 and E13.5 tamoxifen injections respectively), they become progressively more TrPC lineage-biased than at E12, again consistent with previous lineage-tracing analyses (Solar et al., 2009).

In contrast to control pancreata, in E15.5 *Hnf1β-CreER*^{T2}*; R26*$^{dnMaml1\text{-}eGFP}$ pancreata, significantly fewer dnMaml1-eGFP$^+$ cells co-expressed Sox9 following tamoxifen injection at either E12.5 or E13.5 although Sox9$^+$ dnMaml1$^+$ cells were more abundant following the later injection (E12.5 tamoxifen injection: 4.0%-7.3%; E13.5 injection: 10.4%-24.9%)(**Fig. 1K-V**). This resembles the exclusion of Notch-deaf cells from the bipotent progenitor pool seen following tamoxifen injection at E11.5. However, in sharp contrast to dnMaml1$^+$ pancreata exposed to tamoxifen at E11.5 in which 66.3% of dnMaml1-eGFP$^+$ cells were Ptf1a$^+$ (**Fig. 1F,G**), following E12.5 or E13.5 injections, only 20.7% (E12.5) or 11.6% (E13.5) of Notch-deaf cells expressed Ptf1a (**Fig. 1L,M,R,S**). At the expense of this acinar contribution however, ~70% (67.0% chromogranin-A$^+$; 2.4% Ngn3$^+$) and ~80% (72.5%

chromogranin-A$^+$; 7.7% Ngn3$^+$) of dnMaml1-eGFP$^+$ cells contributed to the endocrine compartment following E12.5 or E13.5 tamoxifen injections, respectively, compared with 22.2% of Notch-deaf cells following injection at E11.5 (**Fig. 1I,J,O,P,U,V**). As per an E11.5 tamoxifen injection, following tamoxifen injections at E12.5 or E13.5, significantly fewer dnMaml1-eGFP$^+$ cells in E15.5 *Hnf1β-CreER^{T2}; R26$^{dnMaml1-eGFP}$* pancreata were Ngn3$^+$ (E12.5: 2.4%; E13.5: 7.7%) compared with the 13.0% (E12.5) or 18.6% (E13.5) of YFP$^+$ cells in control *Hnf1β-CreER^{T2}; R26^{YFP}* pancreata (**Fig. 1H-J,N-P,T-V**). This reinforces the notion that sustained dnMaml1 expression in TrPCs is incompatible with an Ngn3$^+$ state, implying that the bulk of the dnMaml1$^+$ cells differentiated shortly after induction of dnMaml1 expression. Moreover, such a large proportion (~70%) of dnMaml1$^+$ cells adopting an endocrine fate following transgene induction from ~E13 (from an E12.5 tamoxifen injection)(**Fig. 1L,M,O,P**), may imply that Notch-deaf *Hnf1β$^+$* progenitors commit to the duct/endocrine-competent TrPC fate before activating *Ngn3* and committing to an endocrine program. Alternatively, dnMaml1 may accelerate the final differentiation step of the newly described endocrine-biased, Ngn3^{Lo} population that appears to be subject to ongoing Notch signaling (Bechard et al., 2016). Thus, the predominant cell fate of dnMaml1$^+$ cells shifts from being acinar to being endocrine after E11.5 and E12.5 tamoxifen injections, respectively (**Fig. 1F,G,I,J,L,M,O,P**). This strongly indicates that Notch blockade from ~E12 renders *Hnf1β$^+$* progenitors unable to contribute to TrPC while Notch abrogation from ~E13 is compatible with TrPC-fate commitment but once allocated to a duct-/endocrine-bipotent progenitor fate, Notch-deaf cells activate an endocrine program. This notion is further supported by the increased contribution of Notch-deaf progenitors to 1) the Sox9$^+$ bipotent progenitor compartment and 2) the Ngn3$^+$ endocrine progenitor population after tamoxifen injection at E13.5 compared with E12.5 (**Fig. 1L,M,O,P,R,S,U,V**). The above results and conclusions on the effects of *Hnf1β*-CreER^{T2}-mediated dnMaml1-EGFP expression upon lineage allocation were independently confirmed by qualitative lineage-tracing analyses in which dnMaml1-eGFP expression was driven by TrPC-specific *Sox9*-CreER^{T2} (Kopp et al., 2011). These showed the same shift in progenitor competence upon blockade of Notch signal reception as described above (**Fig. S1**). Taken together, these findings show that the window through which active Notch signaling is required to commit MPCs to a TrPC fate closes by E13.

Jag1 and Dll1 Expression is Enriched in TiPCs while Notch Activation is TrPC-Specific

Having shown that active Notch signaling is required to allocate MPCs to a TrPC fate until E13, we sought to determine the source of the Notch ligands. To test the hypothesis that signals originate from presumptive TiPCs and their progeny, a comprehensive spatiotemporal expression analysis was conducted for Notch ligands, receptors, and Hes1 in relation to TiPC and TrPC markers during the Notch-dependent PD patterning window as defined by the preceding experiments. IF analysis was used to detect not only endogenous ligands, but also, novel Venus fusion protein reporters for both Jag1 and Dll1 (**Fig. 2A,B**). A previous *in situ*-based survey of Notch pathway components in the developing mouse pancreas revealed that only Notch1 and Notch2 and of the four trans-activating ligands (Jag1, Jag2, Dll1 and Dll4), only Dll1 are expressed in the early (<~E13.5) pancreatic epithelium during PD patterning (Lammert et al., 2000). More recent immunofluorescence studies further revealed Jag1 expression in E10.5 pancreatic epithelium (Nakano et al., 2015). Dll1 expression is first detected in scattered pancreatic epithelial cells at around E9.0 then expands to encompass Ngn3^{+} cells and many MPCs of the E9.5 dorsal pancreas; similar expression is observed in the E10.5 ventral pancreas; between E13.5 and E15.5, Dll1 is expressed in many but not all Ngn3^{+} cells and in nascent acini (Ahnfelt-Rønne et al., 2012; Apelqvist et al., 1999). Previous studies described uniform Jag1 expression in the pancreatic epithelium from E12.5 onwards, as well as in endothelial cells at all stages (Ahnfelt-Rønne et al., 2012; Apelqvist et al., 1999; Golson et al., 2009a; Lammert et al., 2000) with expression then becoming restricted to ducts perinatally (Golson et al., 2009b). More recently, this pancreatic expression pattern of Jag1 was broadly confirmed *via* IF analyses with the exception that uniform Jag1 expression was detected in the pancreatic epithelium from E10.5 (Nakano et al., 2015). Besides Dll1 and Jag1, no other Notch ligand has been described to be expressed in the pancreatic parenchyme. While previous studies have been instrumental in informing our current understanding of Notch ligand expression in the developing pancreas, many bear the caveats that they are reliant upon poorly-validated antisera or dependent upon analysis of transcriptionally-uncoupled surrogate reporters with perdurance far exceeding that of the native ligand protein. In order to circumvent these issues, we employed validated antisera and generated and analyzed novel fusion protein reporters which faithfully recapitulate Jag1 and Dll1 expression. In these novel *Jag1* and *Dll1* alleles (*Jag1*^{J1VmC} and *Dll1*^{D1VmC}, **Fig. 2A,B**), Venus is fused to the C-terminus of Jag1 or Dll1 followed by a self-splicing T2A peptide and mCherry. Using a sensitive rabbit

anti-GFP antibody to detect expression of the Venus fusion proteins, we observed broad, low-level Jag1 expression in E10.5 dorsal pancreas epithelium (MPCs) as well as in the surrounding mesenchyme (**Fig. 2C,E**). Strikingly, by E12.5 prominent Jag1-Venus expression was restricted to distal TiPC cells at the periphery of the epithelium while it was absent from most proximal TrPCs (**Fig. 2D**), revealing Jag1 to be enriched on TiPCs during PD patterning. At E15.5, weak Jag1-Venus expression was detected apically in acinar cells and in non-parenchymal cells, including the vasculature, but expression was excluded from proximal endocrine-/duct-bipotent Sox9^{+} progenitors (**Fig. S3A**). By generating embryos carrying *Jag1*^{J1VmC} and a BAC-transgenic *Hes1-eGFP* reporter (Klinck et al., 2011), we assayed for mCherry as a readout of Jag1 and detected (*Hes1*-)eGFP using a chicken-raised anti-GFP antibody that only detects high levels of GFP/Venus so fails to detect Jag1-Venus. The mCherry reporter is very sensitive, likely due to the long half-life of the cleaved mCherry protein compared to the Venus fusions. Nevertheless, we failed to detect Jag1 expression at E9.5 (**Fig. 2F**), but confirmed the broad, low-level expression in E10.5 dorsal MPCs, many of which co-expressed GFP (**Fig. 2G**). At E11.5 mCherry expression intensified in the distal-most epithelium and was downregulated in proximal epithelium where many mCherry^{-} GFP^{+} cells were evident (**Fig. 2H**). This pattern was reinforced at E12.5 where mCherry expression was largely confined to distal TiPCs (**Fig. 2I**). Notably, GFP^{+} cells were often intercalated within clusters of mCherry^{+} cells at E11.5 and E12.5 (**Fig. 2H, I**), suggesting that Notch activation in these cells is regulated independently of Jag1 expression. mCherry expression was also detected in E15.5 acinar cells but at much reduced levels (**Fig. S3C**).

To confirm the principal finding from the *Jag1*^{J1VmC} expression analysis that Jag1 expression is enriched on TiPCs during Notch-dependent PD patterning, IF was conducted using two independent Jag1 antisera that were validated using *Jag1-null* (Xue et al., 1999) tissue (**Fig. S2A-D''**). Weak Jag1 expression was first detected in the E10.5 dorsal and ventral pancreas (**Fig. 2J** and **Fig. S2A,A'',C,C''**) and by E12.5 during PD patterning when epithelial Jag1 expression was qualitatively higher than at E10.5, it showed a striking restriction to Ptf1a^{+} Nkx6.1^{-} TiPCs, and was clearly excluded from Ptf1a^{-} Nkx6.1^{+} TrPCs (**Fig. 2Q,S,V** and **Fig. S3G-I**). Confirming findings from the *Jag1*^{J1VmC}*; Hes1-*eGFP double-reporter analysis, IF for Hes1 using an antibody validated on *Hes1-null* (Ishibashi et al., 1995) tissue (**Fig. S2G-H''**) revealed nuclear Hes1 expression to be largely restricted to Ptf1a^{-} Nkx6.1^{+} TrPCs at E12.5 (**Fig. 2Q,R,V**) indicating Notch signal transduction to be largely TrPC-specific during

PD patterning. Hes1 expression was strongest in TrPCs adjacent to apices of converging Jag1^{+} TiPC membranes (**Fig. 2Q**). High Hes1 signal was, however, also evident in a few solitary Ptf1a^{+} Nkx6.1^{-} TiPCs expressing Jag1, again indicating that Notch activation in these cells is regulated independently of Jag1 expression (**Fig. 2Q**). Additionally, Jag1 was excluded from the endocrine lineage at all stages examined (**Fig. S3H,K**). Such TiPC-enriched Jag1 expression at E12.5 is discordant with previous reports of uniform pancreatic epithelial Jag1 expression at this stage using anti-Jag1 antisera (Golson et al., 2009a; Nakano et al., 2015). While we cannot fully explain these discrepancies, we suspect they may be related to the low signal-to-noise ratio for anti-Jag1 antibodies.

In contrast to Jag1-Venus, the Dll1-Venus reporter was detected in scattered cells of the E10.5 dorsal pancreas, many of which were Sox9$^{Lo/-}$ (**Fig. 2J,K**). This pattern was maintained at E12.5 with scattered Dll1-Venus^{+} Sox9$^{Lo/-}$ cells in proximal and distal epithelium (**Fig. 2L**). At E15.5 we detected Dll1-Venus expression apically in acinar cells, and in scattered Sox9$^{Lo/-}$ proximal epithelial cells (**Fig. S3B**). Analogous to the *Jag1*^{J1VmC}*; Hes1*-eGFP analysis, we generated and examined *Dll1*^{J1VmC}*; Hes1*-eGFP embryos and, consistent with our previous results (Ahnfelt-Rønne et al., 2012) we detected Dll1-mCherry in scattered cells of the E9.5 dorsal pancreas (**Fig. 2M**). Many mCherry^{+} cells were Sox9$^{Lo/-}$ GFP$^{Lo/-}$ and adjacent to Sox9^{+} GFP^{+} mCherry$^{Lo/-}$ cells (**Fig. 2M**), suggesting the mCherry^{+} cells to be engaged in active signaling. A few cells co-expressed mCherry and GFP, which may be explained by perdurance of mCherry and/or GFP after transcription has ceased. The same pattern was observed at E10.5, E11.5, and E12.5 (**Fig. 2N-P**). At E15.5 many mCherry^{+} cells were found in acini, often interspersed with GFP^{+} cells although the majority of GFP^{+} cells were Sox9^{+} bipotent progenitors (**Fig. S3D-F**). Many proximal cells were mCherry^{Lo} GFP^{Lo}, but Sox9^{-}, possibly representing differentiated endocrine cells with perdurance of the fluorescent proteins.

IF using an anti-Dll1 antibody validated on *Dll1-null* (Hrabe de Angelis et al., 1997) tissue (**Fig. S2E-F''**) confirmed the *Dll1*^{J1VmC} expression analysis). Dll1^{+} cells could be subdivided into several populations. These encompass Dll1^{+} Ptf1a^{+} cells present in the E10.5 pancreas and in E12.5 and E15.5 distal epithelium as well as Dll1^{+} Ngn3^{+} cells, evident at all stages, and Dll1^{+} Ngn3^{-} cells in E12.5 proximal epithelium expressing Nkx6.1 (**Fig. 2R,S,V** and **Fig. S3M-R**). Confirming the *Dll1*^{J1VmC}*; Hes1*-eGFP dual-reporter analysis, Hes1 expression at E12.5 was strongest in those TrPCs adjacent

to Dll^{Hi} cells of the proximal epithelium, suggesting Dll1^{Hi} cells to be actively signaling: Dll1^{Hi} cells tended to be either Hes1^{-} or Hes1^{Lo} (**Fig. 2R**).

IF for both fusion protein reporters and endogenous ligands permitted an examination of ligand co-expression. Consistent with the results described above, a large overlap was observed between Jag1 and Dll1 expression at E10.5 (**Fig. 2E,J**). Some Dll1^{+} Jag1^{-} cells were noted and likely represent Ngn3^{+} cells. Furthermore, a subset of Jag1^{+} TiPCs at E12.5 was Dll1-mCherry^{+} (**Fig. S3E**) and this mosaic Dll1 expression in distal epithelium was retained in E15.5 acinar cells (**Fig. S3F**). IF for Dll1 and Jag1 at E12.5 during PD patterning confirmed the expression of Dll1 in a subset of Jag1^{+} TiPCs (**Fig. 2S,V**).

Finally, as Notch1 and Notch2 were previously detected in the early (<~E13.5) pancreatic epithelium during PD patterning (Lammert et al., 2000), we assayed for their expression at E12.5 using commercially-available antisera. While Notch1 was uniformly expressed in Ptf1a^{+} Nkx6.1^{-} TiPCs and Ptf1a^{-} Nkx6.1^{+} TrPCs (**Fig. 2T**), Notch2 was specifically enriched on TrPCs (**Fig. 2U**).

In sum, these expression analysis findings show two sources of Notch ligand at E12.5 during PD patterning: TiPCs specifically present Jag1 to the most distal TrPC (or TrPC-fated) progenitors while Dll1 is expressed heterogeneously on isolated cells (some Ngn3^{+} endocrine precursors) throughout the epithelium where it is presented to the most proximal TrPCs. Given their largely exclusive Hes1 expression, Notch signal transduction is predominantly TrPC-specific during PD patterning. As Notch1 is expressed on both TiPCs and TrPCs but Notch2 is enriched on the latter, TiPCs bear a higher ligand:receptor ratio than do TrPCs (**Fig. 2V**). Taken together, these results support Notch signal-sending from distal prospective TiPCs and Notch-reception in proximal presumptive TrPCs during PD patterning.

Distal Notch Signals are Required to Specify Terminal Duct Cells

Given the greater abundance of ligand expression on TiPCs concomitant with Notch-dependent TrPC specification, we next functionally tested whether distal cells are the source of Notch signals during this process. To this end, Notch signal-sending was specifically ablated in TiPCs and their descendants *via Ptf1a^{Cre}* (Kawaguchi et al., 2002) -driven recombination of a floxed *Mib1* allele (Koo et al., 2007) (*Mib1$^{\Delta Ptf1a}$*), preventing endocytosis of- and trans-activation by all DSL ligands expressed on Ptf1a^{+} cells (Itoh et al., 2003; Koo et al., 2005; Koo et al., 2007). *Mib1*-depleted cells and their

progeny were identified by recombination of the *R26*^{YFP} reporter allele. While *Ptf1a*^{Cre} is known to be expressed in a subset of MPCs prior to PD patterning and TiPC commitment (Kawaguchi et al., 2002), examination of early (≤E13.5) *Mib1*$^{\Delta Ptf1a}$ pancreata failed to reveal any gross morphological defects (data not shown). Given the profound hypoplasia, precocious endocrine differentiation (dorsal pancreas) and TrPC-to-TiPC fate conversion (ventral pancreas) seen following endoderm-specific recombination of *Mib1-flox* using highly-efficient *Foxa2*^{T2AiCre} (Horn et al., 2012), this lack of dysmorphogenesis in the early *Mib1*$^{\Delta Ptf1a}$ pancreas is consistent with *Ptf1a*^{Cre} activity in MPCs being mosaic, as previously reported (Kawaguchi et al., 2002; Seymour et al., 2012). This is borne out by mosaic YFP labeling from the *R26*^{YFP} reporter allele seen in E13.5 pancreata from *R26*$^{YFP\text{-}\Delta Ptf1a}$ embryos either heterozygous or homozygous for the *Mib1-flox* allele (data not shown). Only efficient deletion of *Mib1* would be expected to manifest in any phenotype since for a cell to be entirely deprived of Notch ligands presented by its neighbors, *Mib1* must be efficiently deleted in all contiguous cells. Likewise, attempts to delete *Mib1* specifically in committed TiPCs from E12 in *Mib1*$^{fl/fl}$ mice carrying the tamoxifen-inducible *Ptf1a*^{CreERTM} allele (Pan et al., 2013) were unsuccessful owing to the inability to obtain sufficiently high recombination efficiency in contiguous TiPCs to exert an effect on adjacent TrPCs (data not shown).

While early development of *Mib1*$^{\Delta Ptf1a}$ pancreata is ostensibly normal, morphogenesis is perturbed later. Analysis at E15.5 revealed the ductal tree to be laterally truncated such that the most distal Sox9^{+} TrPCs/duct cells which normally protrude into the nascent Ptf1a^{+} acini of control pancreata (**Fig. 3A-A''**, arrows), are specifically absent in *Mib1*$^{\Delta Ptf1a}$ embryos (**Fig. 3B-B''**, asterisks). The absence of both DAPI^{+} nuclei (**Fig. 3B**) and YFP-labeled recombined cells (**Fig. 3B,B'**) within the acini supports cell loss as opposed to Sox9 downregulation. Ablation of this specific cell population is consistent with the apical concentration of Dll1 and Jag1 on the adjacent Ptf1a^{+} acinar cells in the secondary transition pancreas (**Fig. S3F,L,R**). It is also concordant with the notion that Notch signaling and, so, the pancreatic program, are only perturbed when *Mib1*, and thus signal-sending, is efficiently ablated. This can occur following multiple rounds of *Ptf1a*^{Cre}-mediated recombination in TiPCs and their acinar progeny in which *Ptf1a*^{Cre} is more robustly expressed compared with MPCs. Given that the most distal Sox9^{+} cells in the secondary transition pancreas are widely accepted to be the precursors of the adult terminal duct/centroacinar (CAC) cells (Beer et al., 2016), this phenotype closely resembles the loss of CAC cells seen following *Ptf1a*^{Cre}-driven double deletion of

Dll1 and *Jag1* (Nakano et al., 2015). Although the distal-most Sox9$^+$ cells are present in E15.5 compound mutants, showing them to be initially specified, reduced survival (decreased proliferation and increased apoptosis) renders them almost undetectable by E18.5 (Nakano et al., 2015). Together, these results suggest that Notch signaling *via* ligands expressed on TiPCs and their acinar progeny is required to support adjacent terminal TrPCs/duct cells.

Mosaic Endodermal Deletion of Dll1 and Jag1 Singly or in Combination Perturbs PD Patterning

Given the abundant epithelial expression of Jag1 and Dll1 during PD patterning (**Fig. 2** and **Fig. S3**), we sought to further investigate the role of these ligands in this process by generating and analyzing a series of mutants in which Jag1 and/or Dll1 were deleted specifically in the endoderm owing to early (<E12) embryonic lethality of global *Jag1*- or *Dll1*-null mice due to hemorrhage (Hrabe de Angelis et al., 1997; Xue et al., 1999). Owing to the close proximity (~5.7 cM) of *Jag1* and *Foxa2* (that we previously used as an efficient Cre driver - (Horn et al., 2012)) on mouse Chromosome 2, generation of mutants with *Foxa2*^{T2AiCre}-mediated recombination of a *Jag1-flox* allele (Kiernan et al., 2006) proved challenging. While protracted breeding to break the linkage between the two alleles was ongoing, *Sox17*^{CreERT2} was used as a driver to generate single and compound endoderm-specific *Jag1/Dll1* mutants. Administration of tamoxifen to pregnant dams at E6.5 (40 µg/g body-weight) resulted in largely endoderm-specific mosaic recombination prior to pancreas specification which was assessed as above *via R26*^{YFP} recombination.

Dll1 deletion by this approach (*Dll1*$^{\Delta Sox17Tam}$) recapitulated our previous findings - *Dll1*$^{\Delta Foxa2}$ mutants showed a decrease in Nkx6.1$^+$ cells at E12.5 (Horn et al., 2012), which recovers by E15.5, suggesting that redundancy from other ligands is able to compensate for the earlier *Dll1* deletion. At E12.5, *Dll1*$^{\Delta Sox17Tam}$ embryos displayed a significant decrease in Ptf1a$^-$ Nkx6.1$^+$ TrPCs (P=0.004), an increase in Ptf1a$^+$ Nkx6.1$^+$ co-expressing cells (P= 0.014), and no change in Ptf1a$^+$ Nkx6.1$^-$ TiPCs compared to controls (**Fig. S4A-B',E-G**), confirming a role for Dll1 in the proper specification of TrPCs. In contrast, Ptf1a$^-$ Nkx6.1$^+$ TrPCs appear to be specified normally in *Jag1*$^{\Delta Sox17Tam}$ embryos. However, Ptf1a$^+$ Nkx6.1$^+$ co-expressing cells were increased in number (P=0.006) at the expense of Ptf1a$^+$ Nkx6.1$^-$ TiPCs although the decrease in the latter just failed to reach statistical significance (P=0.077)(**Fig. S4A,A',C,C',E-G**). Nevertheless, this result is remarkable as it is inconsistent with Jag1 functioning as a classical Notch activator during PD patterning: loss of TrPC-specifying trans-

activating Notch activity would be predicted to reduce the TrPC domain with concomitant TiPC expansion. Rather, the loss of TiPCs suggests that Jag1 is required cell-autonomously to inhibit Notch. As Rbpj directly binds the *Nkx6.1* promoter during PD patterning (Afelik et al., 2012), ectopic Notch activation in TiPCs upon *Jag1* ablation might conceivably directly promote TiPC Nkx6.1 expression accounting for the increased Ptf1a^{+} Nkx6.1^{+} co-positive population observed in the E12.5 *Jag1*$^{\Delta Sox17Tam}$ pancreas.

In relation to single *Dll1*$^{\Delta Sox17Tam}$ and *Jag1*$^{\Delta Sox17Tam}$ mutants, compound *Dll1/Jag1*$^{\Delta Sox17Tam}$ mutants displayed an intermediate phenotype (**Fig. S4A-G**). The decreased proportion of Ptf1a^{+} Nkx6.1^{-} TiPCs failed to reach significance compared to controls or single *Dll1*$^{\Delta Sox17Tam}$ mutants, but neither is it different to that seen in single *Jag1*$^{\Delta Sox17Tam}$ mutants, again likely due to mosaic deletion. However, Ptf1a^{-} Nkx6.1^{+} TrPCs were decreased in number as seen in *Dll1*$^{\Delta Sox17Tam}$ embryos (c.f controls: P=0.023; c.f. *Jag1*$^{\Delta Sox17Tam}$: P=0.016). As for both single mutants, compound *Dll1/Jag1*$^{\Delta Sox17Tam}$ mutants also exhibited an expansion of the Ptf1a^{+} Nkx6-1^{+} co-positive population (P=0.001 compared to controls). Thus, while interpretation of these findings is confounded by the mosaic nature of the ligand deletion, these results show that both Jag1 and Dll1 are required for proper PD patterning by allowing timely resolution of Ptf1a and Nkx6.1 segregation.

Jag1 is Required for Specifying All But the 10% Proximal-Most TrPCs

As described above, after protracted breeding of *Foxa2*^{T2AiCre} and *Jag1-flox* animals, linkage between the two alleles was broken, allowing the generation of *Jag1*$^{+/-}$; *Dll1*$^{fl/+}$; *Foxa2*$^{T2AiCre/T2AiCre}$ mice required for crossing with *Jag1*$^{fl/fl}$; *Dll1*$^{fl/fl}$; *R26*$^{YFP/YFP}$ animals to generate *Foxa2*^{T2AiCre}-driven endoderm-specific compound *Jag1/Dll1* mutants (*Jag1/Dll1*$^{\Delta Foxa2}$). *Jag1*$^{+/-}$; *Dll1*$^{fl/+}$; *Foxa2*$^{T2AiCre/T2AiCre}$ offspring were recovered from parental crosses with significantly lower frequency (3.4%) than the 25% expected from Mendelian inheritance. Thus, we first analyzed pancreata from single *Jag1*$^{\Delta Foxa2}$ mutants obtained *via* similar *flox/null* crosses between *Jag1*$^{+/-}$; *Foxa2*$^{T2AiCre/T2AiCre}$ and *Jag1*$^{fl/fl}$; *R26*$^{YFP/YFP}$ parents. *Jag1*$^{fl/-}$; *R26*$^{YFP/+}$; *Foxa2*$^{T2AiCre/+}$ (*Jag1*$^{\Delta Foxa2}$) mutant and *Jag1*$^{fl/+}$; *R26*$^{YFP/+}$; *Foxa2*$^{T2AiCre/+}$ control offspring were recovered at the expected 1:1 ratio.

Examination of *Jag1*$^{\Delta Foxa2}$ embryos at E10.5 revealed both the dorsal and ventral pancreata to be of normal size and morphology with no evidence of precocious endocrine differentiation (data not shown) despite efficient, near-complete recombination as assessed by *R26*^{YFP} (**Fig. 4A-B'**). This

was mirrored at E12.5 with the *Jag1*$^{\Delta Foxa2}$ mutant pancreas appearing grossly normal in both size and morphology. However, IF analysis revealed the *Jag1*$^{\Delta Foxa2}$ pancreas to be more poorly branched/lobulated than that of littermate controls (**Fig. 4A-B''**). Moreover, the proportion of pancreatic cells expressing Ptf1a (either Nkx6.1^{+} or $^{-}$) was significantly increased (*P*=0.0361) at the expense of a loss of Ptf1a^{-} Nkx6.1^{+} TrPCs (*P*=0.0361) (**Fig. 4A-C**). While Ptf1a expression at E12.5 typically demarcates only the distal-most epithelial cells (**Fig. 4A,A''**) after gradual downregulation from E10.5 when it marks the majority of the MPCs in the epithelium (Kawaguchi et al., 2002; Schaffer et al., 2010), Ptf1a continued to be expressed by *Jag1*$^{\Delta Foxa2}$ pancreatic cells more proximal to this as well as at qualitatively higher levels than in control pancreata (**Fig. 4B,B''**). Thus, as revealed by analysis of *Jag1*$^{\Delta Sox17Tam}$ mutants, Jag1 is required for timely resolution of Ptf1a^{+} Nkx6.1^{+} MPCs into Ptf1a^{+} Nkx6.1^{-} TiPC and Ptf1a^{-} Nkx6.1^{+} TrPC domains.

To assess how the loss of Jag1 ligand impacts Notch signaling during PD patterning, we assayed for Hes1 in *Jag1*$^{\Delta Foxa2}$ pancreata given inconsistent IF detection of cleaved N1ICD in our hands. This revealed that while Hes1 expression and, so, active Notch transduction, is normally largely confined to TrPCs at E12.5 (**Fig. 2I,P,Q,R,V** and **Fig. 4D**), Hes1 IF signal was upregulated in the distal-most epithelial cells of the E12.5 *Jag1*$^{\Delta Foxa2}$ pancreas (**Fig. 4E,F**). Thus, loss of Jag1 in TiPCs during PD patterning results in increased Notch activity in these cells. This is consistent with the above proposal that Jag1 is required cell-autonomously to inhibit Notch in TiPC cells. It is not implausible to think that without this delineation between Notch^{Lo} distal cells and Notch^{Hi} proximal cells, segregation of MPCs into TiPC and TrPC cells respectively is unable to proceed.

By assaying for Ptf1a and either Nkx6.1 or Sox9 for TrPC/bipotent endocrine-duct-competent progenitors, we determined that resolution into distinct Ptf1a^{+} Nkx6.1^{-} distal and Ptf1a^{-} Nkx6.1^{+} proximal domains does not occur until E14.5 in the *Jag1*$^{\Delta Foxa2}$ pancreas, two days later than normal (**Fig. S5A-D,G-J**). Through this stage, endocrine differentiation, as assessed on the basis of Ngn3^{+} endocrine precursors and insulin^{+} β-cell numbers, appears ostensibly unaffected (**Fig. S5E,F,K,L**) and data not shown). By E15.5 however, delayed PD patterning in the *Jag1*$^{\Delta Foxa2}$ pancreas manifests in a striking ~85% decrease (*P*=0.0003) in Nkx6.1^{+} cells relative to control littermates (**Fig. 5A-C**) despite gross morphology and pancreas size remaining largely unaffected (**Fig. 5I-J'**). As Nkx6.1 expression defines both endocrine-/duct-bipotent progenitors ("ducts") and β-cells in the secondary transition pancreas, we assayed for Sox9 and insulin respectively to distinguish between these two cell types.

This analysis revealed a dramatic ~90% reduction (*P*<0.0001) in Sox9$^+$ cells and a two-fold decrease (*P*=0.0062) in insulin$^+$ β-cells in the E15.5 *Jag1*$^{\Delta Foxa2}$ mutant *versus* littermate control pancreas (**Fig. 5D-F**). Both section and wholemount IF analysis revealed only the proximal-most Sox9$^+$ cells to be retained in the mutant pancreas (**Fig. 5E,H,J,J'**). This suggests that Jag1 is required for specifying ~90% of TrPCs with the remainder induced Jag1-independently *via* other ligand(s) most likely expressed in the proximal epithelium. Delayed PD patterning and failure to specify the majority of the TrPC population manifests in severe dysmorphogenesis of the ductal tree: mirroring Sox9, ductal cells marked by Hnf1β and DBA are reduced in the E15.5 *Jag1*$^{\Delta Foxa2}$ pancreas, to be found only in the proximal-most epithelium (data not shown). This phenotype resembles a far more severe ductal paucity than that previously shown *via* mosaic *Jag1* deletion in the early pancreas (Golson et al., 2009a; Golson et al., 2009b). Perhaps most strikingly, despite the severe depletion of the ductal tree, the cytoarchitecture of the acinar and the overall pancreas is largely unaffected in the absence of *Jag1*. Acinar structure is largely maintained and acinar cells express mature acinar markers including Ptf1a, Mist1, amylase and CPA1 in the E15.5 and E18.5 *Jag1*$^{\Delta Foxa2}$ pancreas (**Fig. 5B,H,L**, **Fig. S6B,C,E,F,H,I,K,L** and **Fig. S7D**). This is despite acini being isolated from Sox9$^+$ duct cells: even when discontinuous ducts occur in E15.5 mutants, they often terminate prematurely and are not "capped" by a Ptf1a$^+$ nascent acinus as in control littermates (**Fig. 5G,H**). In addition, elongated duct-like structures can be morphologically identified in the proximal epithelium E15.5 *Jag1*$^{\Delta Foxa2}$ pancreata which express Ptf1a (and Mist1), not Sox9 (**Fig. 5H,L**). Concordant with maintenance of acinar architecture despite ductal paucity, apicobasal polarity (as assessed by expression of Muc1, ZO-1 and PKCζ) is maintained in the E15.5 *Jag1*$^{\Delta Foxa2}$ pancreas (**Fig. S6A-F'**). By E18.5, just prior to birth (and the latest stage that mutants could be recovered due to neonatal lethality), *Jag1*$^{\Delta Foxa2}$ pancreata were still equivalent in size to those of control littermates (**Fig. S7**). Endocrine cell depletion was prominent, especially so for later-arising somatostatin$^+$ δ-cells, consistent with a more pronounced lack of endocrine-/duct-competent bipotent progenitors during later pancreas development (**Fig. S7B**). While paucity of the ductal tree, as assessed by IF for Muc1, Cytokeratin 19 (CK19) and DBA, was obvious, "ring"-like structures expressing both acinar (amylase and CPA1) as well as ductal (CK19) markers, were widespread throughout the E18.5 *Jag1*$^{\Delta Foxa2}$ pancreatic epithelium (**Fig. S6I,I',L,L'** and **Fig. S7D,F**). While this is consistent with acinar-to-ductal metaplasia,

genetic lineage-tracing approaches to specifically label acinar cells in the *Jag1* mutant will be required to test this.

Jag1 and Dll1 Specify Endocrine-/Duct-Competent TrPCs

As mentioned above, while ~90% of TrPCs are lost in the *Jag1*$^{\Delta Foxa2}$ mutant, the remaining ~10% proximal-most TrPCs are specified in a Jag1-independent manner, most likely by a ligand(s) expressed in the vicinity. With Dll1 comprising the most likely candidate, we crossed *Jag1*$^{+/-}$*; Dll1*$^{fl/+}$*; Foxa2*$^{T2AiCre/T2AiCre}$ with *Jag1*$^{fl/fl}$*; Dll1*$^{fl/fl}$*; R26*$^{YFP/YFP}$ mice to generate *Foxa2*^{T2AiCre}-driven endoderm-specific compound *Jag1/Dll1* mutants (*Jag1/Dll1*$^{\Delta Foxa2}$). With only three (all female) *Jag1*$^{+/-}$*; Dll1*$^{fl/+}$*; Foxa2*$^{T2AiCre/T2AiCre}$ parent animals obtained amongst 89 offspring to date (3.4% actual recovery *versus* 25% expected), three E15.5 litters were harvested of 13 embryos in total comprising two *Jag1/Dll1*$^{\Delta Foxa2}$ compound mutants (25% chance of obtaining this genotype given Mendelian inheritance).

In order to compare *Jag1*$^{\Delta Foxa2}$ mutants with compound *Jag1/Dll1*$^{\Delta Foxa2}$, we also generated single *Dll1*$^{\Delta Foxa2}$ mutant and control mice without ligand deletions (*Foxa2*^{T2AiCre}*; R26*^{YFP}). Analysis of all four genotypes at E15.5 revealed no change in the numbers of Ptf1a^{+} cells or Nkx6.1^{+} cells between single *Dll1*$^{\Delta Foxa2}$ mutant and control pancreata at E15.5 while, as above, Nkx6.1^{+} cells were severely depleted in *Jag1*$^{\Delta Foxa2}$ mutants (P=0.0002) with a concordant expansion in Ptf1a^{+} cells (P=0.0085) (**Fig. 6A,B,E,I**). Both compound *Jag1/Dll1*$^{\Delta Foxa2}$ mutants examined mirrored the other in exhibiting a more profound loss of Nkx6.1^{+} cells (P=0.0014) and increase in Ptf1a^{+} cells (P=0.0056) than either single mutant (**Fig. 6F,I**). Almost all Nkx6.1^{+} cells were ablated from every tissue section, except for those at the site of the main duct. Similar to Nkx6.1^{+} cells, Sox9^{+} cell numbers were unchanged between E15.5 *Dll1*$^{\Delta Foxa2}$ and control pancreata while they were severely reduced in *Jag1*$^{\Delta Foxa2}$ mutants (P<0.0001) (**Fig. 6C,D,G,J**). Again, compound *Jag1/Dll1*$^{\Delta Foxa2}$ mutants exhibited a more profound decrease in Sox9^{+} cells (P=0.0003) than either single mutant (**Fig. 6H,J**). Numbers of insulin^{+} β-cells were reduced in both E15.5 *Dll1*$^{\Delta Foxa2}$ and *Jag1*$^{\Delta Foxa2}$ mutants relative to controls (P=0.0083 and P=0.0003 respectively) while compound *Jag1/Dll1*$^{\Delta Foxa2}$ mutants exhibited a more profound loss (P<0.0001) than either single mutant alone (**Fig. 6C,D,G,H,K**). Thus, given that the near-complete ablation of TrPC derivatives in embryos lacking both Jag1 and Dll1 phenocopies *Mib1*$^{\Delta Foxa2}$ mice lacking all Notch signal-sending ability (Horn et al., 2012), it can be argued that the

remaining 10% of TrPCs specified in *Jag1*$^{\Delta Foxa2}$ embryos are specified by Dll1 cues provided by proximal epithelial cells. It was recently shown that the pancreatic ducts in zebrafish are specified by Jagged1b (Jag1b) and Jagged2b (Jag2b) (Zhang et al., 2017). Our findings hereby show that their function in mammals is served by Jag1 and Dll1. We show that these ligands are expressed respectively on distal TiPCs and more proximal epithelium during PD patterning in the mouse with Jag1 specifying the majority of the ductal tree (Jag1) and the 10% of proximal-most TrPCs being specified by proximal epithelial Dll1 cues.

Multiple sources of Notch ligands are important to ensure proper PD patterning of the developing pancreas epithelium prior to E13 and suggest that the distal-most TrPCs receive Notch ligand input from TiPCs while more centrally located TrPCs receive Notch ligand input from Ngn3^{+} endocrine precursors.

Materials & Methods

Mice

Published mouse strains used herein include: *R26*$^{dnMaml1\text{-}eGFP}$ (Horn et al., 2012), *Gt(ROSA)26Sortm1(EYFP)Cos* (*R26*^{YFP} (Srinivas et al., 2001)), *Mib1*^{tm2Kong} (*Mib1*^{fl} (Koo et al., 2007)), *Dll1*^{tm1Gos} (*Dll1*^{LacZ} (Hrabe de Angelis et al., 1997)), *Dll1*$^{tm1.1Hri}$ (*Dll1*^{fl} (Horn et al., 2012)), *Jag1*^{tm1Grid} (*Jag1*$^{-}$ (Xue et al., 1999)), *Jag1*^{tm2Grid} (*Jag1*^{fl} (Kiernan et al., 2006)), *TgHes1eGFP*^{1Hri} (*Hes1-eGFP* (Klinck et al., 2011)), *Hes1*^{tm1Fgu} (*Hes1*$^{-}$ (Ishibashi et al., 1995)), *Foxa2*^{T2AiCre} (Horn et al., 2012), *Hnf1β*-CreER^{T2} (Solar et al., 2009), *Sox9*-CreER^{T2} (Kopp et al., 2011), *Ptf1a*^{Cre} (Kawaguchi et al., 2002) and *Ptf1a*^{CreERTM} (Pan et al., 2013). Transgenic reporters for Dll1 (*Dll1*^{D1VmC}) and Jag1 (*Jag1*^{J1VmC}) were generated in the lab of Ryoichiro Kageyama (**Fig. 2A,B**), and were maintained as heterozygotes due to hypomorphic effects of the Dll1-Venus fusion protein. D1VmC genotyping primers: Fwd: 5′ CTTCAAAGGACACCAAGTACCAGTCG 3′, WT-Rev: 5′ CTGTCCATAGTGCAATGGGAACAACC 3′, Venus-Rev: 5′ CTTGCTCACCATAAAGATGCGACCTCC 3′, wt: 409bp, tg: 211bp. J1VmC genotyping primers: Fwd: 5′ CAACACGGTCCCCATTAAGGATTACGAG 3′, WT-Rev: 5′ CTGTCCATAGTGCAATGGGAACAACC 3′, Venus-Rev: as above, wt: 469bp, tg: 211bp. *Sox17*^{CreERT2} was generated by cassette exchange of the *Sox17-LCA* allele (Choi et al., 2012). Genotyping primers: Fwd: 5′-TGCCACGACCAAGTGACAGC-3′, Rev: 5′-CCAGGTTACGGATATAGTTCATG-3′, tg: 6-700bp. Deletion by *Foxa2*^{T2AiCre} is denoted by $^{\Delta Foxa2}$, *Sox17*^{CreERT2} deletion by $^{\Delta Sox17Tam}$ and *Ptf1a*^{Cre} deletion by $^{\Delta Ptf1a}$. Transgenic animals carrying only one copy of *Sox17*^{CreERT2} were used as controls in

the ligand deletion experiments. Midday on the day of vaginal plug appearance was considered E0.5. Tamoxifen (Sigma) was dissolved at 10 mg/ml in corn oil (Sigma) and a single dose of 75 μg/g (for *Hnf1β-/Sox9*-CreER^{T2}-mediated *R26*$^{dnMaml1\text{-}eGFP/YFP}$ induction) or 40 μg/g (for *Sox17*^{CreERT2}-mediated ligand deletion) body-weight administered by intraperitoneal injection at noon ± 1 hour. All animal experiments described herein were conducted in accordance with European legislation and authorized by the Danish Regulatory Authority.

Histology and Immunofluorescence Analysis

Dissected whole embryos (E10.5-E12.5) and foregut preparations (E13.5-E18.5) were fixed in 4% paraformaldehyde in PBS, cryoembedded in Tissue-Tek O.C.T. (Sakura Finetek) and sectioned at 10 μm. For immunofluorescence analysis, antigen retrieval was conducted in pH6.0 citrate buffer, followed by permeabilization in 0.15% Triton X-100 in PBS. After blocking in 1% normal donkey serum in PBS with 0.1% Tween-20, sections were incubated overnight at 4°C with primary antibodies (listed in **Table S1**) diluted in the same buffer. Primary antibodies were detected with anti-rabbit, guinea pig, mouse, rat, goat, sheep or chicken donkey-raised secondary antibodies conjugated to either Cy5 (1:500), Cy3 (1:1,000), Alexa Fluor 488 (1:1,000) or DyLight 405 (1:200) (all Jackson ImmunoResearch Laboratories). Slides were mounted in Vectashield (Vector Laboratories) with or without DAPI for counterstaining nuclei. Whole-mount IF of E15.5 foregut preparations was performed as previously described (Ahnfelt-Ronne et al., 2007) for Muc1 (Armenian hamster MH1 (CT2); Invitrogen; 1:500) and Sox9 (guinea pig; Ole Madsen, Novo Nordisk/BCBC; 1:2,000). Specimens were cleared with BABB (benzyl alcohol:benzyl benzoate 1:2) then *z*-stack image scanned. Images were captured on a Leica SP8 (or Zeiss LSM780 for whole-mount specimens) confocal microscope and figures prepared using Adobe Photoshop/Illustrator CS6 (Adobe Systems, San Jose, CA, USA).

Cell Quantification and Statistical Analyses

Determination of cell fate of lineage-traced eGFP- (*R26*$^{dnMaml1\text{-}GFP}$) or YFP- (*R26*^{YFP}) labeled cells was assessed manually for a minimum of 200 cells per antibody combination per embryo on every fifth section. For E12.5 *Dll1*$^{\Delta Sox17Tam}$, *Jag1*$^{\Delta Sox17Tam}$, *Dll1/Jag1*$^{\Delta Sox17Tam}$ and *Jag1*$^{\Delta Foxa2}$ analysis, numbers of Ptf1a^{+} Nkx6.1^{-}, Ptf1a^{-} Nkx6.1^{+} and Ptf1a^{+} Nkx6.1^{+} cells were manually scored on every fifth section

using Imaris. For quantification of E12.5 *Jag1*$^{\Delta Foxa2}$ Hes1 IF signal intensity in distal-most Ptf1a^{+} cells relative to background, corrected total cell fluorescence (CTCF) was determined using FIJI (Burgess et al., 2010; McCloy et al., 2014). Numbers of Ptf1a^{+} Nkx6.1^{-}, Ptf1a^{-} Nkx6.1^{+} and Ptf1a^{+} Nkx6.1^{+} cells as well as Sox9^{+} cells and insulin^{+} cells were manually scored from every tenth section of dorsal pancreas from E15.5 control, *Jag1*$^{\Delta Foxa2}$, *Dll1*$^{\Delta Foxa2}$ and *Jag1/Dll1*$^{\Delta Foxa2}$ embryos and expressed relative to mm^{2} (*R26*)YFP^{+} dorsal pancreatic epithelium using FIJI. Data were analyzed using the Student *t* test using 2-tailed analysis (GraphPad). Data are presented as mean $\pm$ S.D.

Acknowledgements

We thank Young-Yun Kong for *Mib1*^{fl} mice, Jorge Ferrer for *Hnf1β*-CreERT2 mice, Heiko Lickert for *Foxa2*^{T2AiCre} mice, Chris Wright for *Ptf1a*^{Cre} and *Ptf1a*^{CreERTM} lines, Anne Grapin-Botton and Mark A. Magnuson for *Sox17*^{CreERT2} mice and Ole D. Madsen and Jane E. Johnson for antibodies.

Competing Interests

The authors declare no competing or financial interests.

Author Contributions

P.A.S. designed, carried out experiments and wrote the manuscript. C.A.C. designed, carried out *Jag1*^{J1VmC} and *Dll1*^{D1VmC} expression analysis and *Sox17*^{CreERT2}-mediated double ligand deletions and co-wrote the manuscript. M.C.J. contributed to *Jag1*$^{\Delta Foxa2}$ phenotypic analysis. I.I. and R.K. generated the *Jag1*^{J1VmC} and *Dll1*^{D1VmC} mouse lines while A.G-B. and M.A.M. generated the *Sox17*^{CreERT2} line. P.S. designed the experiments and wrote the manuscript. All authors revised the manuscript.

Funding

This work has been supported by the Faculty of Health and Medical Sciences, University of Copenhagen, The NNF Danish Stem Cell Center (DanStem, http://danstem.ku.dk/) and Novo Nordisk Foundation grants [Nordic endocrinology 16076 and 10717]. The Novo Nordisk Foundation Center for Stem Cell Biology is supported by a Novo Nordisk Foundation grant number NNF17CC0027852.

References

Afelik, S., Qu, X., Hasrouni, E., Bukys, M. A., Deering, T., Nieuwoudt, S., Rogers, W., Macdonald, R. J. and Jensen, J. (2012). Notch-mediated patterning and cell fate allocation of pancreatic progenitor cells. *Development* **139**, 1744-1753.

Ahn, S. and Joyner, A. L. (2004). Dynamic changes in the response of cells to positive hedgehog signaling during mouse limb patterning. *Cell* **118**, 505-516.

Ahnfelt-Ronne, J., Jorgensen, M. C., Hald, J., Madsen, O. D., Serup, P. and Hecksher-Sorensen, J. (2007). An improved method for three-dimensional reconstruction of protein expression patterns in intact mouse and chicken embryos and organs. *J Histochem Cytochem* **55**, 925-930.

Ahnfelt-Rønne, J., Jørgensen, M. C., Klinck, R., Jensen, J. N., Füchtbauer, E., Deering, T., MacDonald, R. J., Wright, C. V., Madsen, O. D. and Serup, P. (2012). Ptf1a-mediated control of Dll1 reveals an alternative to the lateral inhibition mechanism. *Development* **139**, 33-45.

Apelqvist, A., Li, H., Sommer, L., Beatus, P., Anderson, D. J., Honjo, T., Hrabe de Angelis, M., Lendahl, U. and Edlund, H. (1999). Notch signalling controls pancreatic cell differentiation. *Nature* **400**, 877-881.

Bankaitis, E. D., Bechard, M. E. and Wright, C. V. (2015). Feedback control of growth, differentiation, and morphogenesis of pancreatic endocrine progenitors in an epithelial plexus niche. *Genes Dev* **29**, 2203-2216.

Bechard, M. E., Bankaitis, E. D., Hipkens, S. B., Ustione, A., Piston, D. W., Yang, Y. P., Magnuson, M. A. and Wright, C. V. (2016). Precommitment low-level Neurog3 expression defines a long-lived mitotic endocrine-biased progenitor pool that drives production of endocrine-committed cells. *Genes Dev* **30**, 1852-1865.

Beer, R. L., Parsons, M. J. and Rovira, M. (2016). Centroacinar cells: At the center of pancreas regeneration. *Dev Biol* **413**, 8-15.

Bray, S. J. (2016). Notch signalling in context. *Nat Rev Mol Cell Biol* **17**, 722-735.

Burgess, A., Vigneron, S., Brioudes, E., Labbe, J. C., Lorca, T. and Castro, A. (2010). Loss of human Greatwall results in G2 arrest and multiple mitotic defects due to deregulation of the cyclin B-Cdc2/PP2A balance. *Proc Natl Acad Sci U S A* **107**, 12564-12569.

Chapman, G., Sparrow, D. B., Kremmer, E. and Dunwoodie, S. L. (2011). Notch inhibition by the ligand DELTA-LIKE 3 defines the mechanism of abnormal vertebral segmentation in spondylocostal dysostosis. *Hum Mol Genet* **20**, 905-916.

Choi, E., Kraus, M. R., Lemaire, L. A., Yoshimoto, M., Vemula, S., Potter, L. A., Manduchi, E., Stoeckert, C. J., Jr., Grapin-Botton, A. and Magnuson, M. A. (2012). Dual lineage-specific expression of Sox17 during mouse embryogenesis. *Stem cells (Dayton, Ohio)* **30**, 2297-2308.

Cras-Meneur, C., Li, L., Kopan, R. and Permutt, M. A. (2009). Presenilins, Notch dose control the fate of pancreatic endocrine progenitors during a narrow developmental window. *Genes Dev* **23**, 2088-2101.

Danielian, P. S., Muccino, D., Rowitch, D. H., Michael, S. K. and McMahon, A. P. (1998). Modification of gene activity in mouse embryos in utero by a tamoxifen-inducible form of Cre recombinase. *Curr Biol* **8**, 1323-1326.

Geffers, I., Serth, K., Chapman, G., Jaekel, R., Schuster-Gossler, K., Cordes, R., Sparrow, D. B., Kremmer, E., Dunwoodie, S. L., Klein, T., et al. (2007). Divergent functions and distinct localization of the Notch ligands DLL1 and DLL3 in vivo. *J Cell Biol* **178**, 465-476.

Golson, M. L., Le Lay, J., Gao, N., Bramswig, N., Loomes, K. M., Oakey, R., May, C. L., White, P. and Kaestner, K. H. (2009a). Jagged1 is a competitive inhibitor of Notch signaling in the embryonic pancreas. *Mech Dev* **126**, 687-699.

Golson, M. L., Loomes, K. M., Oakey, R. and Kaestner, K. H. (2009b). Ductal malformation and pancreatitis in mice caused by conditional Jag1 deletion. *Gastroenterology* **136**, 1761-1771 e1761.

Gradwohl, G., Dierich, A., LeMeur, M. and Guillemot, F. (2000). neurogenin3 is required for the development of the four endocrine cell lineages of the pancreas. *Proc Natl Acad Sci U S A* **97**, 1607-1611.

Grapin-Botton, A., Majithia, A. R. and Melton, D. A. (2001). Key events of pancreas formation are triggered in gut endoderm by ectopic expression of pancreatic regulatory genes. *Genes Dev* **15**, 444-454.

Gu, G., Dubauskaite, J. and Melton, D. A. (2002). Direct evidence for the pancreatic lineage: NGN3+ cells are islet progenitors and are distinct from duct progenitors. *Development* **129**, 2447-2457.

Hald, J., Sprinkel, A. E., Ray, M., Serup, P., Wright, C. and Madsen, O. D. (2008). Generation and characterization of Ptf1a antiserum and localization of Ptf1a in relation to Nkx6.1 and Pdx1 during the earliest stages of mouse pancreas development. *J Histochem Cytochem* **56**, 587-595.

High, F. A., Lu, M. M., Pear, W. S., Loomes, K. M., Kaestner, K. H. and Epstein, J. A. (2008). Endothelial expression of the Notch ligand Jagged1 is required for vascular smooth muscle development. *Proc Natl Acad Sci U S A* **105**, 1955-1959.

High, F. A., Zhang, M., Proweller, A., Tu, L., Parmacek, M. S., Pear, W. S. and Epstein, J. A. (2007). An essential role for Notch in neural crest during cardiovascular development and smooth muscle differentiation. *J Clin Invest* **117**, 353-363.

Horn, S., Kobberup, S., Jorgensen, M. C., Kalisz, M., Klein, T., Kageyama, R., Gegg, M., Lickert, H., Lindner, J., Magnuson, M. A., et al. (2012). Mind bomb 1 is required for pancreatic beta-cell formation. *Proc Natl Acad Sci U S A* **109**, 7356-7361.

Hrabe de Angelis, M., McIntyre, J., 2nd and Gossler, A. (1997). Maintenance of somite borders in mice requires the Delta homologue DII1. *Nature* **386**, 717-721.

Ishibashi, M., Ang, S. L., Shiota, K., Nakanishi, S., Kageyama, R. and Guillemot, F. (1995). Targeted disruption of mammalian hairy and Enhancer of split homolog-1 (HES-1) leads to up-regulation of neural helix-loop-helix factors, premature neurogenesis, and severe neural tube defects. *Genes Dev* **9**, 3136-3148.

Itoh, M., Kim, C. H., Palardy, G., Oda, T., Jiang, Y. J., Maust, D., Yeo, S. Y., Lorick, K., Wright, G. J., Ariza-McNaughton, L., et al. (2003). Mind bomb is a ubiquitin ligase that is essential for efficient activation of Notch signaling by Delta. *Dev Cell* **4**, 67-82.

Jensen, J., Pedersen, E. E., Galante, P., Hald, J., Heller, R. S., Ishibashi, M., Kageyama, R., Guillemot, F., Serup, P. and Madsen, O. D. (2000). Control of endodermal endocrine development by Hes-1. *Nat Genet* **24**, 36-44.

Kawaguchi, Y., Cooper, B., Gannon, M., Ray, M., MacDonald, R. J. and Wright, C. V. (2002). The role of the transcriptional regulator Ptf1a in converting intestinal to pancreatic progenitors. *Nat Genet* **32**, 128-134.

Kesavan, G., Sand, F. W., Greiner, T. U., Johansson, J. K., Kobberup, S., Wu, X., Brakebusch, C. and Semb, H. (2009). Cdc42-mediated tubulogenesis controls cell specification. *Cell* **139**, 791-801.

Kiernan, A. E., Xu, J. and Gridley, T. (2006). The Notch ligand JAG1 is required for sensory progenitor development in the mammalian inner ear. *PLoS Genet* **2**, e4.

Klinck, R., Fuchtbauer, E. M., Ahnfelt-Ronne, J., Serup, P., Jensen, J. N. and Jorgensen, M. C. (2011). A BAC transgenic Hes1-EGFP reporter reveals novel expression domains in mouse embryos. *Gene expression patterns : GEP* **11**, 415-426.

Koo, B. K., Lim, H. S., Song, R., Yoon, M. J., Yoon, K. J., Moon, J. S., Kim, Y. W., Kwon, M. C., Yoo, K. W., Kong, M. P., et al. (2005). Mind bomb 1 is essential for generating functional Notch ligands to activate Notch. *Development* **132**, 3459-3470.

Koo, B. K., Yoon, M. J., Yoon, K. J., Im, S. K., Kim, Y. Y., Kim, C. H., Suh, P. G., Jan, Y. N. and Kong, Y. Y. (2007). An obligatory role of mind bomb-1 in notch signaling of mammalian development. *PLoS One* **2**, e1221.

Kopinke, D., Brailsford, M., Shea, J. E., Leavitt, R., Scaife, C. L. and Murtaugh, L. C. (2011). Lineage tracing reveals the dynamic contribution of Hes1+ cells to the developing and adult pancreas. *Development* **138**, 431-441.

Kopp, J. L., Dubois, C. L., Schaffer, A. E., Hao, E., Shih, H. P., Seymour, P. A., Ma, J. and Sander, M. (2011). Sox9+ ductal cells are multipotent progenitors throughout development but do not produce new endocrine cells in the normal or injured adult pancreas. *Development* **138**, 653-665.

Ladi, E., Nichols, J. T., Ge, W., Miyamoto, A., Yao, C., Yang, L. T., Boulter, J., Sun, Y. E., Kintner, C. and Weinmaster, G. (2005). The divergent DSL ligand Dll3 does not activate Notch signaling but cell autonomously attenuates signaling induced by other DSL ligands. *J Cell Biol* **170**, 983-992.

Lammert, E., Brown, J. and Melton, D. A. (2000). Notch gene expression during pancreatic organogenesis. *Mech Dev* **94**, 199-203.

Magenheim, J., Klein, A. M., Stanger, B. Z., Ashery-Padan, R., Sosa-Pineda, B., Gu, G. and Dor, Y. (2011). Ngn3(+) endocrine progenitor cells control the fate and morphogenesis of pancreatic ductal epithelium. *Dev Biol* **359**, 26-36.

Maillard, I., Koch, U., Dumortier, A., Shestova, O., Xu, L., Sai, H., Pross, S. E., Aster, J. C., Bhandoola, A., Radtke, F., et al. (2008). Canonical notch signaling is dispensable for the maintenance of adult hematopoietic stem cells. *Cell Stem Cell* **2**, 356-366.

Maillard, I., Weng, A. P., Carpenter, A. C., Rodriguez, C. G., Sai, H., Xu, L., Allman, D., Aster, J. C. and Pear, W. S. (2004). Mastermind critically regulates Notch-mediated lymphoid cell fate decisions. *Blood* **104**, 1696-1702.

McCloy, R. A., Rogers, S., Caldon, C. E., Lorca, T., Castro, A. and Burgess, A. (2014). Partial inhibition of Cdk1 in G 2 phase overrides the SAC and decouples mitotic events. *Cell Cycle* **13**, 1400-1412.

Nakano, Y., Negishi, N., Gocho, S., Mine, T., Sakurai, Y., Yazawa, M., Abe, K., Yagita, H., Habu, S., Kageyama, R., et al. (2015). Disappearance of centroacinar cells in the Notch ligand-deficient pancreas. *Genes Cells* **20**, 500-511.

Offield, M. F., Jetton, T. L., Labosky, P. A., Ray, M., Stein, R. W., Magnuson, M. A., Hogan, B. L. and Wright, C. V. (1996). PDX-1 is required for pancreatic outgrowth and differentiation of the rostral duodenum. *Development* **122**, 983-995.

Ohlsson, H., Karlsson, K. and Edlund, T. (1993). IPF1, a homeodomain-containing transactivator of the insulin gene. *EMBO J* **12**, 4251-4259.

Pan, F. C., Bankaitis, E. D., Boyer, D., Xu, X., Van de Casteele, M., Magnuson, M. A., Heimberg, H. and Wright, C. V. (2013). Spatiotemporal patterns of multipotentiality in Ptf1a-expressing cells during pancreas organogenesis and injury-induced facultative restoration. *Development* **140**, 751-764.

Schaffer, A. E., Freude, K. K., Nelson, S. B. and Sander, M. (2010). Nkx6 transcription factors and Ptf1a function as antagonistic lineage determinants in multipotent pancreatic progenitors. *Dev Cell* **18**, 1022-1029.

Seymour, P. A., Shih, H. P., Patel, N. A., Freude, K. K., Xie, R., Lim, C. J. and Sander, M. (2012). A Sox9/Fgf feed-forward loop maintains pancreatic organ identity. *Development* **139**, 3363-3372.

Shih, H. P., Kopp, J. L., Sandhu, M., Dubois, C. L., Seymour, P. A., Grapin-Botton, A. and Sander, M. (2012). A Notch-dependent molecular circuitry initiates pancreatic endocrine and ductal cell differentiation. *Development* **139**, 2488-2499.

Shimojo, H. and Kageyama, R. (2016). Oscillatory control of Delta-like1 in somitogenesis and neurogenesis: A unified model for different oscillatory dynamics. *Semin Cell Dev Biol* **49**, 76-82.

Solar, M., Cardalda, C., Houbracken, I., Martin, M., Maestro, M. A., De Medts, N., Xu, X., Grau, V., Heimberg, H., Bouwens, L., et al. (2009). Pancreatic exocrine duct cells give rise to insulin-producing beta cells during embryogenesis but not after birth. *Dev Cell* **17**, 849-860.

Srinivas, S., Watanabe, T., Lin, C. S., William, C. M., Tanabe, Y., Jessell, T. M. and Costantini, F. (2001). Cre reporter strains produced by targeted insertion of EYFP and ECFP into the ROSA26 locus. *BMC Dev Biol* **1**, 4.

Tu, L., Fang, T. C., Artis, D., Shestova, O., Pross, S. E., Maillard, I. and Pear, W. S. (2005). Notch signaling is an important regulator of type 2 immunity. *J Exp Med* **202**, 1037-1042.

Villasenor, A., Chong, D. C., Henkemeyer, M. and Cleaver, O. (2010). Epithelial dynamics of pancreatic branching morphogenesis. *Development* **137**, 4295-4305.

Wang, S., Yan, J., Anderson, D. A., Xu, Y., Kanal, M. C., Cao, Z., Wright, C. V. and Gu, G. (2010). Neurog3 gene dosage regulates allocation of endocrine and exocrine cell fates in the developing mouse pancreas. *Dev Biol* **339**, 26-37.

Wessells, N. K. and Cohen, J. H. (1967). Early Pancreas Organogenesis: Morphogenesis, Tissue Interactions, and Mass Effects. *Dev Biol* **15**, 237-270.

Xue, Y., Gao, X., Lindsell, C. E., Norton, C. R., Chang, B., Hicks, C., Gendron-Maguire, M., Rand, E. B., Weinmaster, G. and Gridley, T. (1999). Embryonic lethality and vascular defects in mice lacking the Notch ligand Jagged1. *Hum Mol Genet* **8**, 723-730.

Zhang, D., Gates, K. P., Barske, L., Wang, G., Lancman, J. J., Zeng, X. I., Groff, M., Wang, K., Parsons, M. J., Crump, J. G., et al. (2017). Endoderm Jagged induces liver and pancreas duct lineage in zebrafish. *Nat Commun* **8**, 769.

Zhou, Q., Law, A. C., Rajagopal, J., Anderson, W. J., Gray, P. A. and Melton, D. A. (2007). A multipotent progenitor domain guides pancreatic organogenesis. *Dev Cell* **13**, 103-114.

Figure Legends

Figure 1. The Window of Notch-Dependent TrPC Allocation Closes by E13. (**A,B**) Tamoxifen (Tam) administration to experimental mice induces *Hnf1β-CreER*^{T2}-mediated expression of a dnMaml1-GFP fusion protein from the *R26* locus, rendering *Hnf1β*$^{+}$ TrPC-biased MPCs and their progeny permanently Notch-insensitive and GFP-labeled (**A**) while in control embryos, the same cell population is YFP-labeled but remains Notch signaling-intact following tamoxifen-induced *Hnf1β-CreER*^{T2}-mediated recombination of the *R26*^{YFP} reporter (**B**). (**C**) Approximate temporal windows of Tam activity resulting from single intraperitoneal (i.p.) injections at E11.5, E12.5 or E13.5: pancreata were analysed at E15.5 whereupon cell fate of labeled TrPCs and their progeny was assessed on the basis of marker expression (**D**). Scale bar = 50 μm.

Figure 2. Expression of Jag1 and Dll1 in the Developing Pancreas. (**A,B**) Schematics showing the structure of *Jag1*^{J1VmC} (**A**) and *Dll1*^{D1VmC} (**B**) fusion protein reporters. (**C-E**) Sections of E10.5 (**C,E**) and E12.5 (**D**) *Jag1*^{J1VmC} embryos stained for the Jag1-Venus fusion protein and Sox9 (and Dll1, **E**). Sections of E9.5 (**F**), E10.5 (**G**), E11.5 (**H**), and E12.5 (**I**) *Jag1*^{J1VmC} embryos stained for Jag1-mCherry, GFP (from Hes1-eGFP), and Sox9. (**J-L**) Sections of E10.5 (**J,K**) and E12.5 (**L**) *Dll1*^{D1VmC} embryos stained for the Dll1-Venus fusion protein and Sox9 (and Jag1, **J**). Sections of E9.5 (**M**), E10.5 (**N**), E11.5 (**O**), and E12.5 (**P**) *Dll1*^{D1VmC} embryos stained for Dll1-mCherry, GFP (from Hes1-eGFP), and Sox9. (**Q1-S5**) Serial sections of E12.5 *wild-type* pancreas stained for the TiPC marker Ptf1a and TrPC marker Nkx6.1 and either Jag1 and Hes1 (**Q1-Q5**), Dll1 and Hes1 (**R1-R5**) or Jag1 and Dll1 (**S1-S5**). (**T1-U3**) Serial sections of E12.5 *wild-type* pancreas stained for Ptf1a and Nkx6.1 and either Notch1 (**T1-T3**) or Notch2 (**U1-U3**). (**V**) Schematic summarizing expression patterns of Jag1, Dll1 and Hes1 with relation to Ptf1a^{+} TiPCs, Nkx6.1^{+} TrPCs and Ngn3^{+} endocrine precursors in the E12.5 pancreas. See also **Supplemental Figure 3**

Figure 3. Distal Notch Signaling is Required to Specify Terminal Duct Cells. In control E15.5 pancreata, the branched ductal tree (Sox9^{+}) extends distally to the periphery of the pancreatic epithelium (predominantly YFP-labeled *via Ptf1a*^{Cre}-mediated *R26*^{YFP} recombination), with terminal duct cells juxtaposed with and distal to Ptf1a^{+} acinar cells (**A,A',A''**; arrows in high-power insets of

boxed fields). Such terminal duct cells are, however, specifically absent from littermate *Ptf1a*^{Cre}*; Mib1*$^{fl/fl}$*; R26*^{YFP} mutant pancreata (**B,B',B''**; asterisks in insets). Scale bar = 100 μm.

Figure 4. Failure of TiPC and TrPC Markers to Resolve in E12.5 *Jag1*$^{\Delta Foxa2}$ Pancreas is Associated with Hes1 Upregulation in the Distal-Most TiPCs. (**A-B''**) IF for Ptf1a, Nkx6.1 and YFP on E12.5 control and *Jag1*$^{\Delta Foxa2}$ pancreata. Highly efficient *R26*^{YFP} recombination is evident throughout the pancreatic epithelium (**A-B'**) and as for **A''** and **B''**, the YFP channel is omitted from subsequent figures for clarity. While Ptf1a marks only the distal-most epithelial cells (TiPCs) in E12.5 control littermates (**A,A''**), qualitatively higher levels of Ptf1a are expressed more proximally within the *Jag1*$^{\Delta Foxa2}$ pancreas (**B,B''**). This is reflected in increased proportions of Ptf1a^{+} (Nkx6.1$^{+/-}$) cells (*P*=0.0361) at the expense of a loss of (Ptf1a^{-}) Nkx6.1^{+} TrPCs (*P*=0.0361) in the E12.5 *Jag1*$^{\Delta Foxa2}$ pancreas (**C**). (**D-E**) IF for Ptf1a and Hes1 reveals Hes1 to be upregulated in the distal-most Ptf1a^{+} TiPCs (asterisks) in *Jag1*$^{\Delta Foxa2}$ mutants (**E**) compared with control littermates (**D**). Quantification of corrected total cell fluorescence (CTCF) of Hes1 IF signal in distal-most Ptf1a^{+} cells reveals increased signal (*P*<0.0001) in *Jag1*$^{\Delta Foxa2}$ mutants (**F**).

Figure 5. Ductal Paucity and β-Cell Depletion Result From *Jag1* Deletion While the Acinar Program is Unperturbed. (**A-C**) IF for Ptf1a and Nkx6.1 reveals Nkx6.1^{+} TrPC-derived duct and β-cells to be ~85% reduced (*P*=0.0003) in E15.5 *Jag1*$^{\Delta Foxa2}$ mutants (**B,C**) relative to control littermates (**A**): only the proximal-most Nkx6.1^{+} cells are retained (**B**). Concordantly, TrPC-derived Sox9^{+} endocrine-/duct-bipotent progenitors and insulin^{+} β-cells are ~90% (*P*<0.0001) and ~50% (*P*=0.0062) reduced in E15.5 *Jag1*$^{\Delta Foxa2}$ *versus* control pancreata (**D-F**). Despite ~90% duct loss, Ptf1a^{+} acinar architecture is retained in the E15.5 *Jag1*$^{\Delta Foxa2}$ pancreas: apicobasal polarity is intact with Muc1 decorating acini apically (**H**). However, "isolated" acini are evident in the mutant (**H**) with no juxtaposed Sox9^{+} cells "capped" by acini as in controls (**G**). Muc1 is retained apically throughout the E15.5 *Jag1*$^{\Delta Foxa2}$ acinar pancreas (**J**), revealing comparable size and gross morphology to control littermates (**I**). However, while Sox9 marks the entire ductal tree in control E15.5 embryos (**I'**), only the distal-most Sox9^{+} duct cells are retained in mutants (**J'**). Mist1, a marker of acinar identity, is co-expressed with Ptf1a in E15.5 *Jag1*$^{\Delta Foxa2}$ acinar cells (**L**) as in control pancreas (**K**) but Ptf1a^{+} Mist1^{+} elongated "duct"-like structures are evident in the proximal *Jag1*$^{\Delta Foxa2}$ pancreatic epithelium (**L**, upper inset). Regions of

the dorsal pancreas shown in **I'** and **J'** (optical sections of whole-mount specimens) are represented by boxed regions in **I** and **J** (maximum intensity projections) respectively.

Figure 6. While Jag1 Specifies 90% of TrPC-derived Duct Cells, Dll1 Induces the Proximal-Most Remainder. IF for Ptf1a and Nkx6.1 reveals no change in ratio between *Dll1*$^{\Delta Foxa2}$ and control pancreata at E15.5 while Nkx6.1^{+} cells are severely depleted in *Jag1*$^{\Delta Foxa2}$ mutants (*P*=0.0002) with a concordant increase in Ptf1a^{+} cells (*P*=0.0085); compound *Jag1/Dll1*$^{\Delta Foxa2}$ mutants exhibit a more profound loss of Nkx6.1^{+} cells (*P*=0.0014) and gain of Ptf1a^{+} cells (*P*=0.0056) than either single mutant (**A,B,E,F,I**). Similarly, Sox9^{+} cell numbers are unchanged between E15.5 *Dll1*$^{\Delta Foxa2}$ and control pancreata while they are severely reduced in *Jag1*$^{\Delta Foxa2}$ mutants (*P*<0.0001); compound *Jag1/Dll1*$^{\Delta Foxa2}$ mutants exhibit a more profound decrease in Sox9^{+} cells (*P*=0.0003) than either single mutant (**C,D,G,H,J**). Numbers of insulin^{+} β-cells are reduced in both E15.5 *Dll1*$^{\Delta Foxa2}$ and *Jag1*$^{\Delta Foxa2}$ mutants relative to controls (*P*=0.0083 and *P*=0.0003 respectively) while compound *Jag1/Dll1*$^{\Delta Foxa2}$ mutants exhibit a more profound loss (*P*<0.0001) than either single mutant (**C,D,G,H,K**). Note: significant *P* values were not displayed for Ptf1a^{+} Nkx6.1^{+} cells in **I** for clarity.

Figure 1

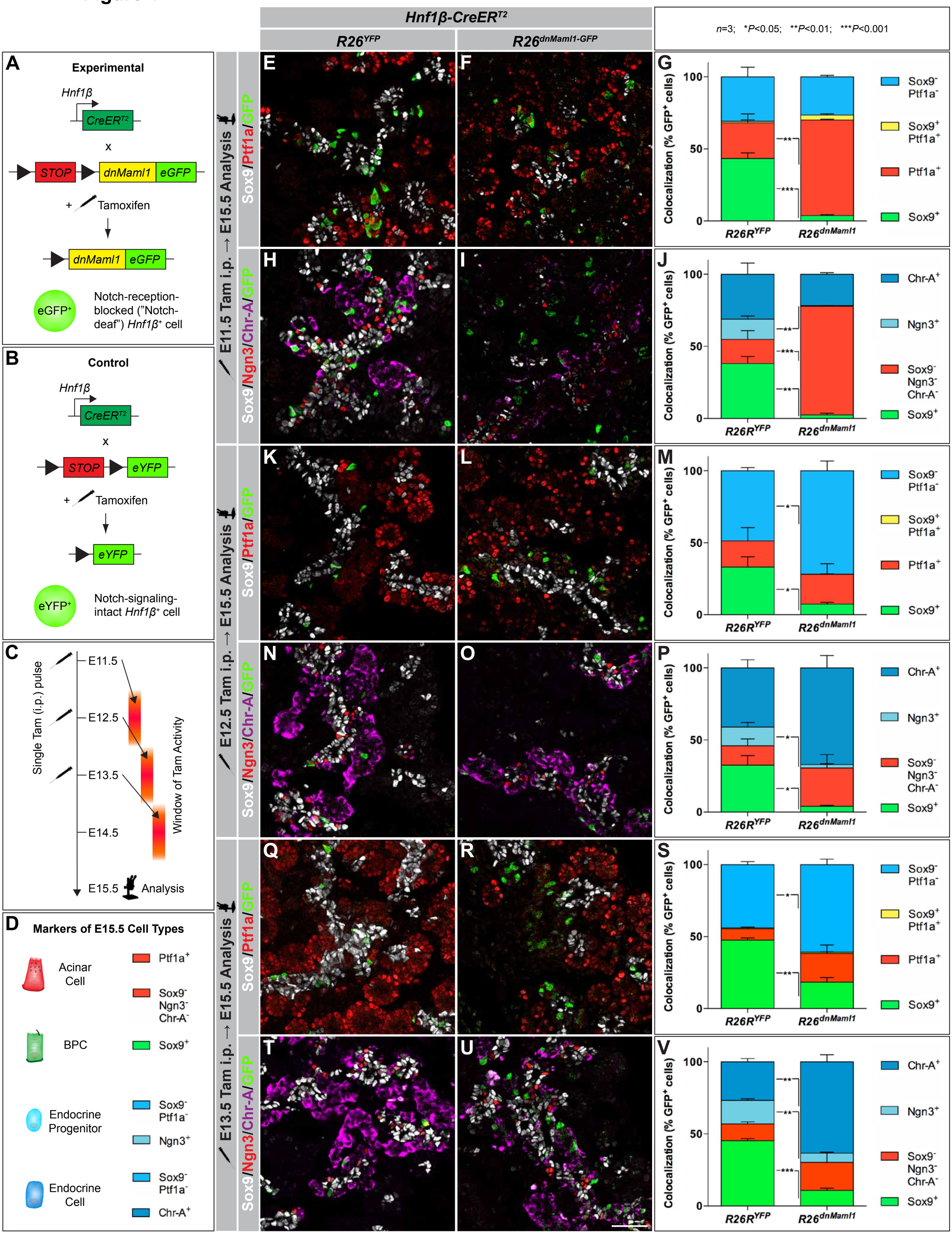
Hnf1β-CreER^{T2}
R26^{YFP}
R26$^{dnMaml1-GFP}$
n=3; *P<0.05; **P<0.01; ***P<0.001
A
Experimental
Hnf1β
CreER^{T2}
x
STOP
dnMaml1
eGFP
+ Tamoxifen
dnMaml1
eGFP
eGFP+
Notch-reception-blocked ("Notch-deaf") Hnf1β+ cell
B
Control
Hnf1β
CreER^{T2}
x
STOP
eYFP
+ Tamoxifen
eYFP
eYFP+
Notch-signaling-intact Hnf1β+ cell
C
Single Tam (i.p.) pulse
E11.5
E12.5
E13.5
E14.5
E15.5
Analysis
Window of Tam Activity
D
Markers of E15.5 Cell Types
Acinar Cell
Ptf1a+
BPC
Sox9- Ngn3- Chr-A-
Sox9+
Endocrine Progenitor
Sox9- Ptf1a-
Ngn3+
Endocrine Cell
Sox9- Ptf1a-
Chr-A+
E11.5 Tam i.p. → E15.5 Analysis
E12.5 Tam i.p. → E15.5 Analysis
E13.5 Tam i.p. → E15.5 Analysis
Sox9/Ptf1a/GFP
Sox9/Ngn3/Chr-A/GFP
E
F
H
I
K
L
N
O
Q
R
T
U
G
J
M
P
S
V
Colocalization (% GFP+ cells)
100
50
0
R26R^{YFP}
R26^{dnMaml1}
Sox9- Ptf1a-
Sox9+ Ptf1a+
Ptf1a+
Sox9+
Chr-A+
Ngn3+
Sox9- Ngn3- Chr-A-
**
***
*

Figure 2

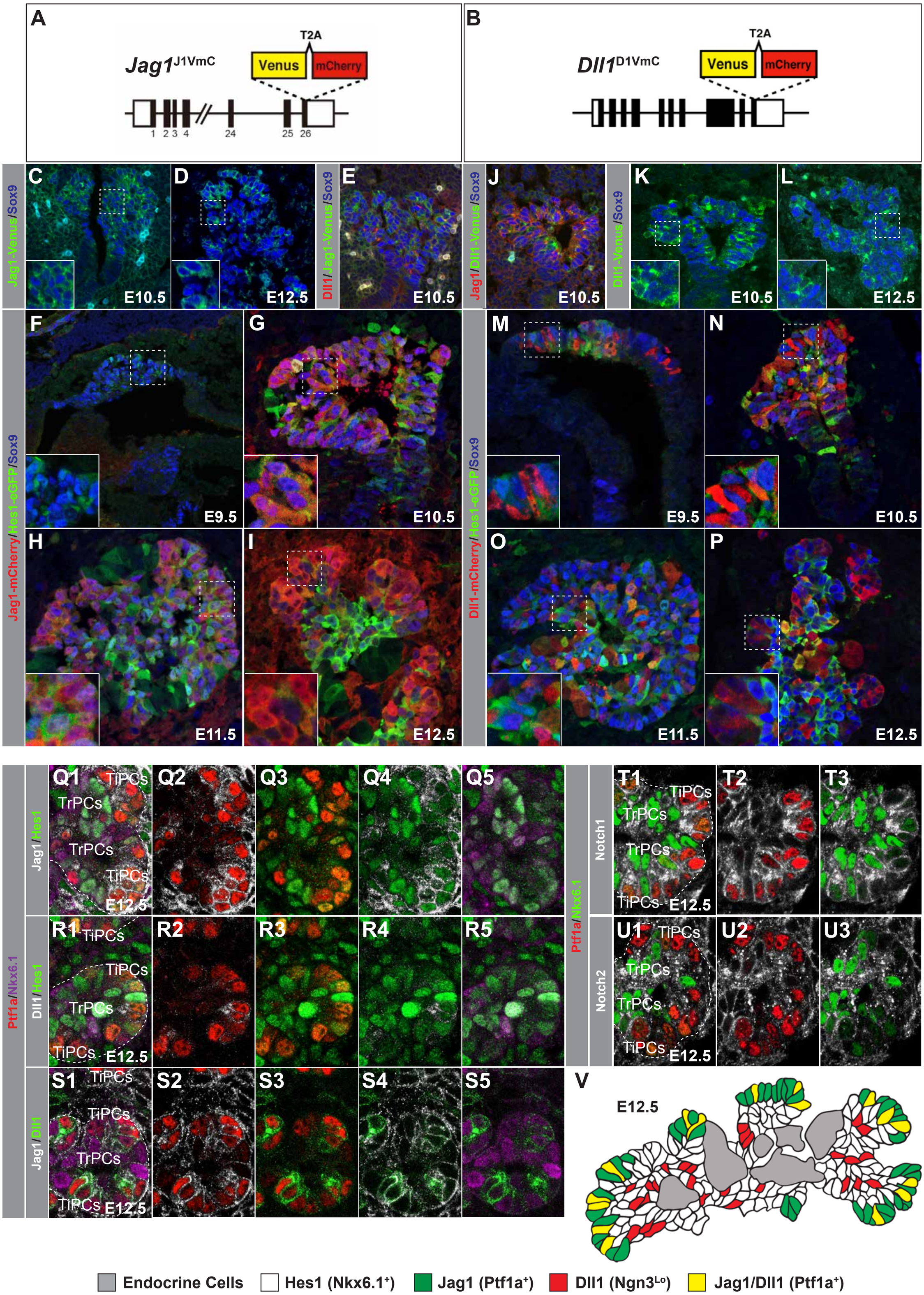
A
Jag1J1VmC
T2A
Venus
mCherry
1 2 3 4
24
25 26
B
Dll1D1VmC
T2A
Venus
mCherry
Jag1-Venus/Sox9
C
E10.5
D
E12.5
Dll1/Jag1-Venus/Sox9
E
E10.5
Jag1/Dll1-Venus/Sox9
J
E10.5
Dll1-Venus/Sox9
K
E10.5
L
E12.5
Jag1-mCherry/Hes1-eGFP/Sox9
F
E9.5
G
E10.5
H
E11.5
I
E12.5
Dll1-mCherry/Hes1-eGFP/Sox9
M
E9.5
N
E10.5
O
E11.5
P
E12.5
Ptf1a/Nkx6.1
Jag1/Hes1
Q1
TiPCs
TrPCs
TrPCs
TiPCs
E12.5
Q2
Q3
Q4
Q5
Dll1/Hes1
R1
TiPCs
TiPCs
TrPCs
TiPCs
E12.5
R2
R3
R4
R5
Jag1/Dll1
S1
TiPCs
TiPCs
TrPCs
TiPCs
E12.5
S2
S3
S4
S5
Ptf1a/Nkx6.1
Notch1
T1
TiPCs
TrPCs
TrPCs
TiPCs
E12.5
T2
T3
Notch2
U1
TiPCs
TrPCs
TrPCs
TiPCs
E12.5
U2
U3
V
E12.5
Endocrine Cells
Hes1 (Nkx6.1+)
Jag1 (Ptf1a+)
Dll1 (Ngn3Lo)
Jag1/Dll1 (Ptf1a+)

Figure 3

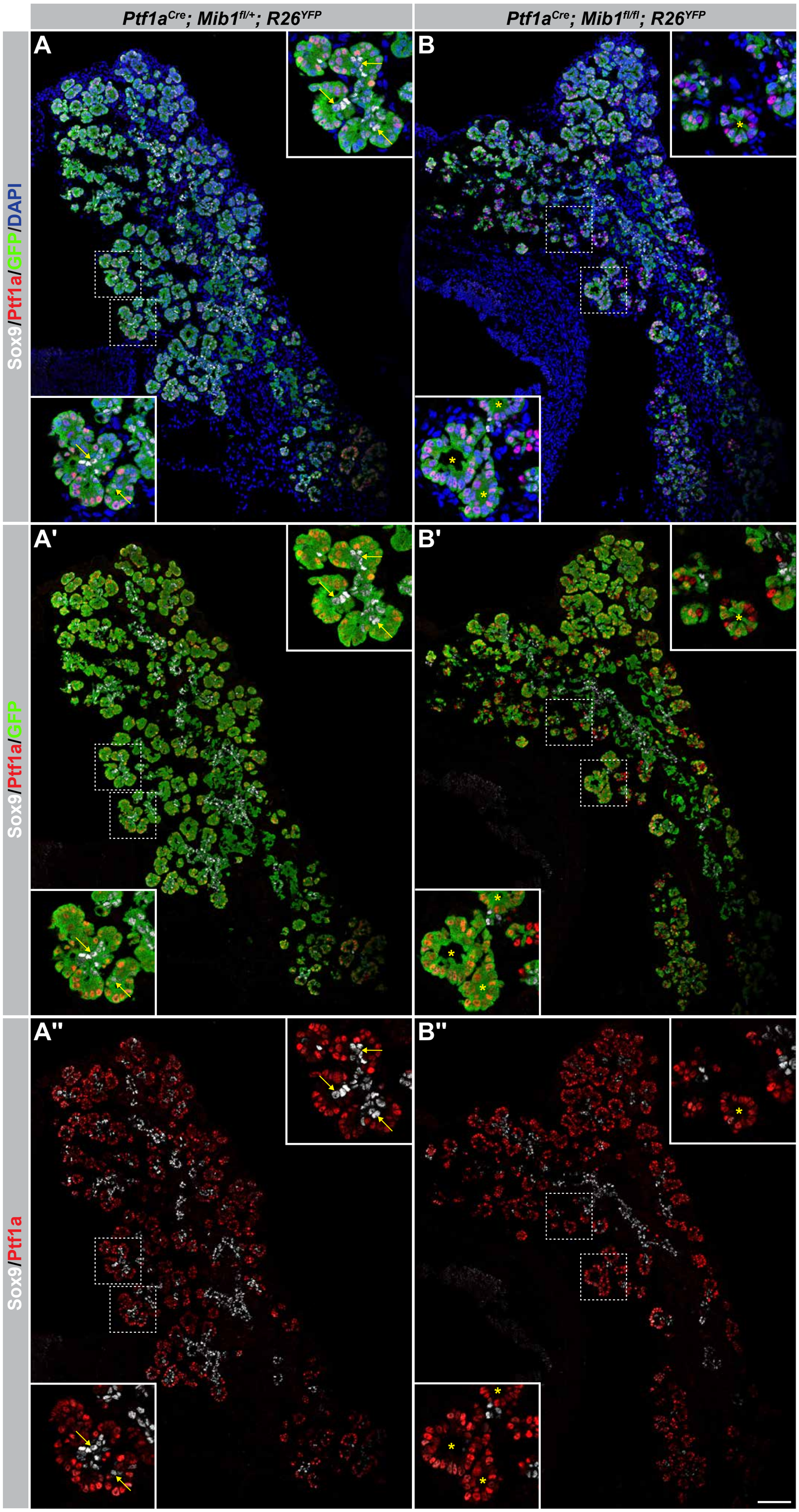
Ptf1a^Cre; Mib1^fl/+; R26^YFP
Ptf1a^Cre; Mib1^fl/fl; R26^YFP
Sox9/Ptf1a/GFP/DAPI
Sox9/Ptf1a/GFP
Sox9/Ptf1a
A
B
A'
B'
A"
B"

Figure 4

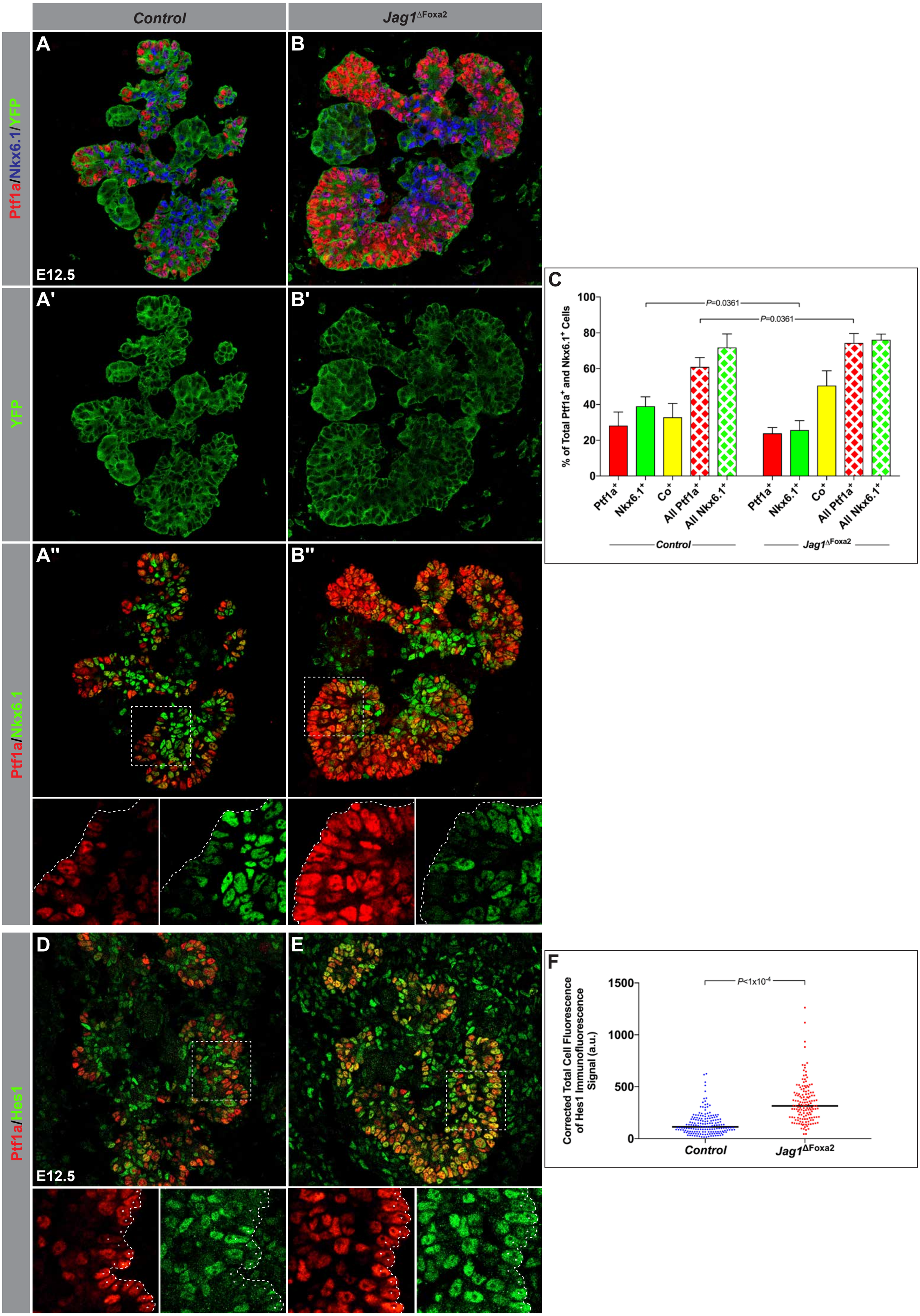
Control
Jag1ΔFoxa2
Ptf1a/Nkx6.1/YFP
YFP
Ptf1a/Nkx6.1
Ptf1a/Hes1
A
B
A'
B'
A''
B''
D
E
E12.5
C
% of Total Ptf1a+ and Nkx6.1+ Cells
P=0.0361
P=0.0361
Ptf1a+
Nkx6.1+
Co+
All Ptf1a+
All Nkx6.1+
Control
Jag1ΔFoxa2
F
Corrected Total Cell Fluorescence of Hes1 Immunofluorescence Signal (a.u.)
P<1x10-4
Control
Jag1ΔFoxa2

Figure 5

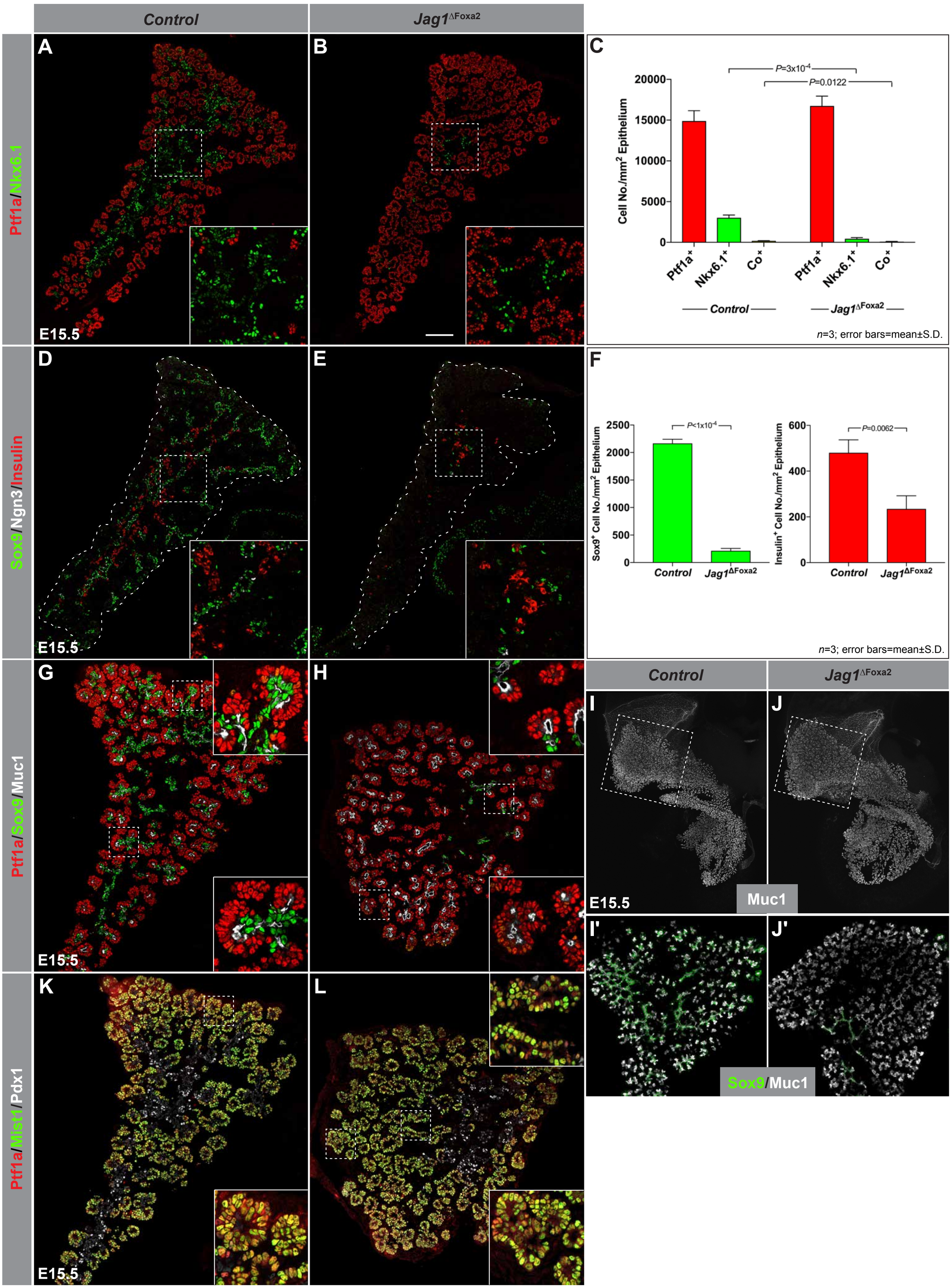
Control
Jag1ΔFoxa2
A
B
C
Ptf1a/Nkx6.1
E15.5
P=3x10-4
P=0.0122
Cell No./mm2 Epithelium
20000
15000
10000
5000
0
Ptf1a+
Nkx6.1+
Co+
Control
Jag1ΔFoxa2
n=3; error bars=mean±S.D.
D
E
F
Sox9/Ngn3/Insulin
P<1x10-4
P=0.0062
Sox9+ Cell No./mm2 Epithelium
Insulin+ Cell No./mm2 Epithelium
2500
2000
1500
1000
500
600
400
200
G
H
I
J
Ptf1a/Sox9/Muc1
Muc1
I'
J'
Sox9/Muc1
K
L
Ptf1a/Mist1/Pdx1

Figure 6

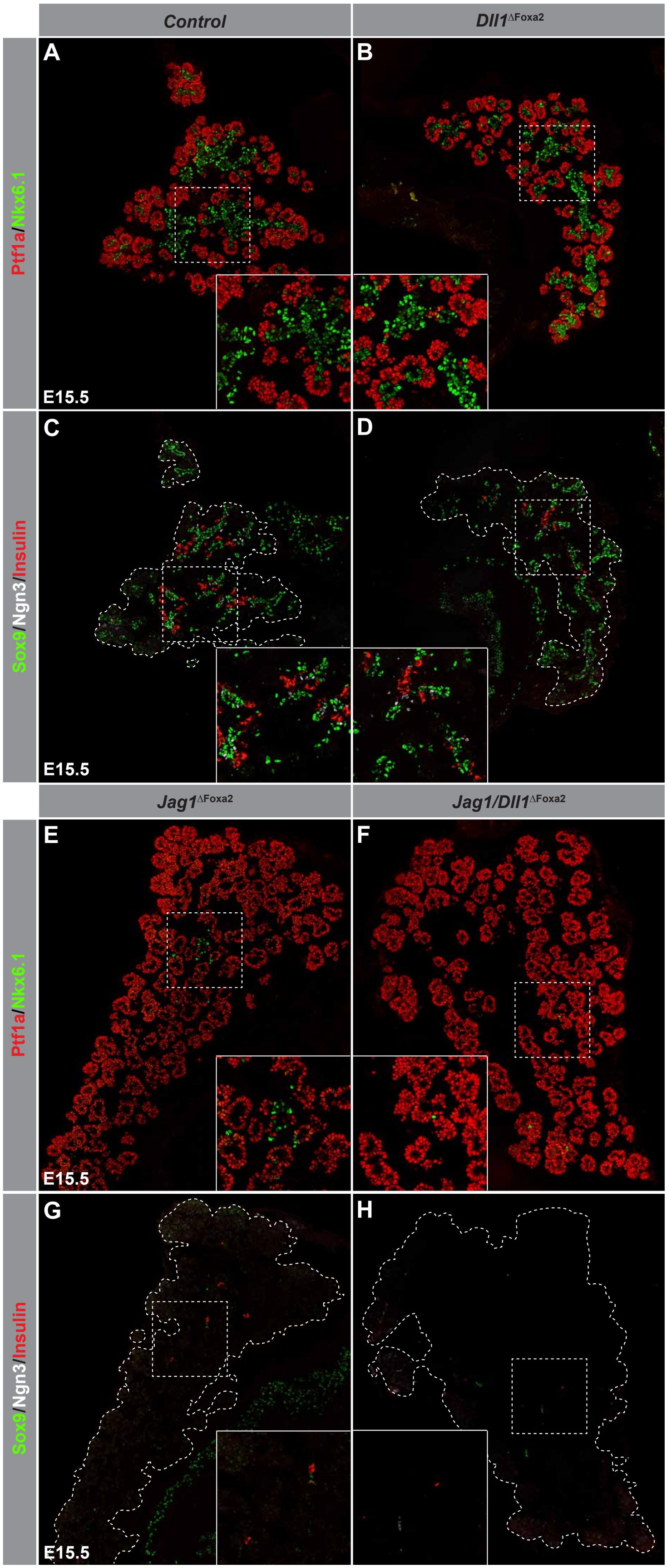

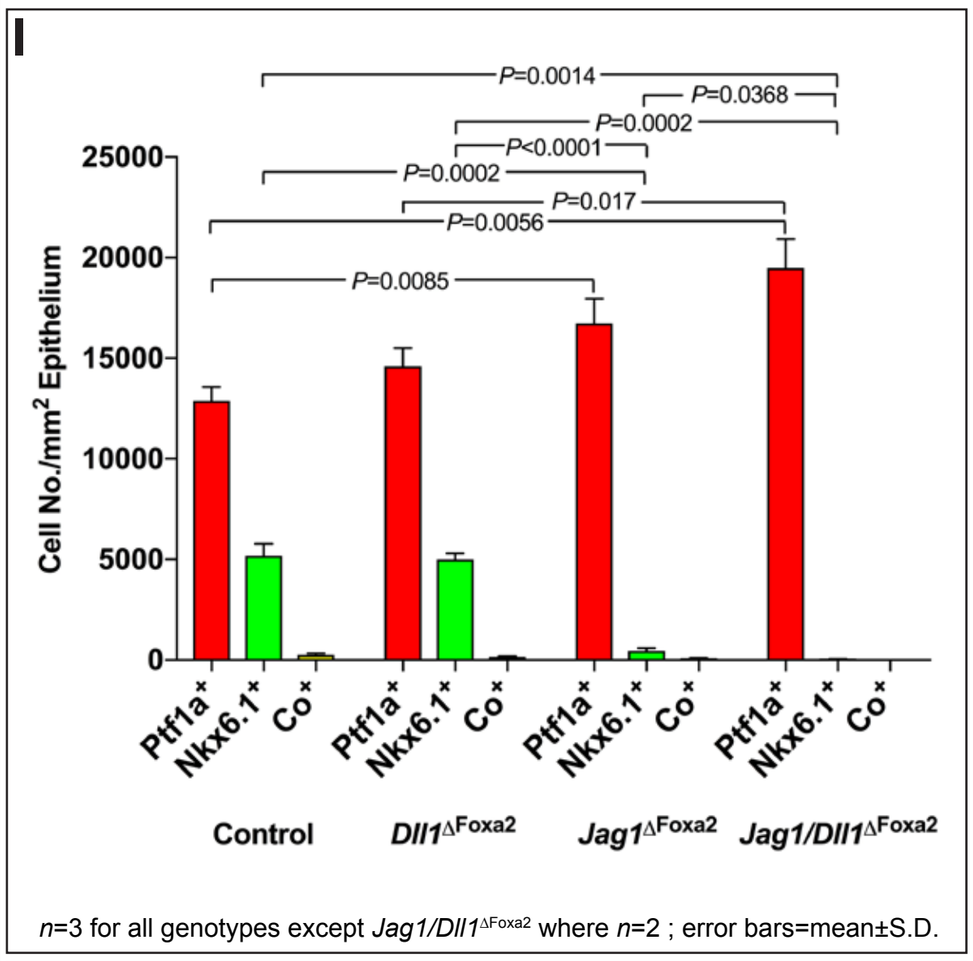

n=3 for all genotypes except *Jag1/Dll1*$^{\Delta Foxa2}$ where *n*=2 ; error bars=mean±S.D.

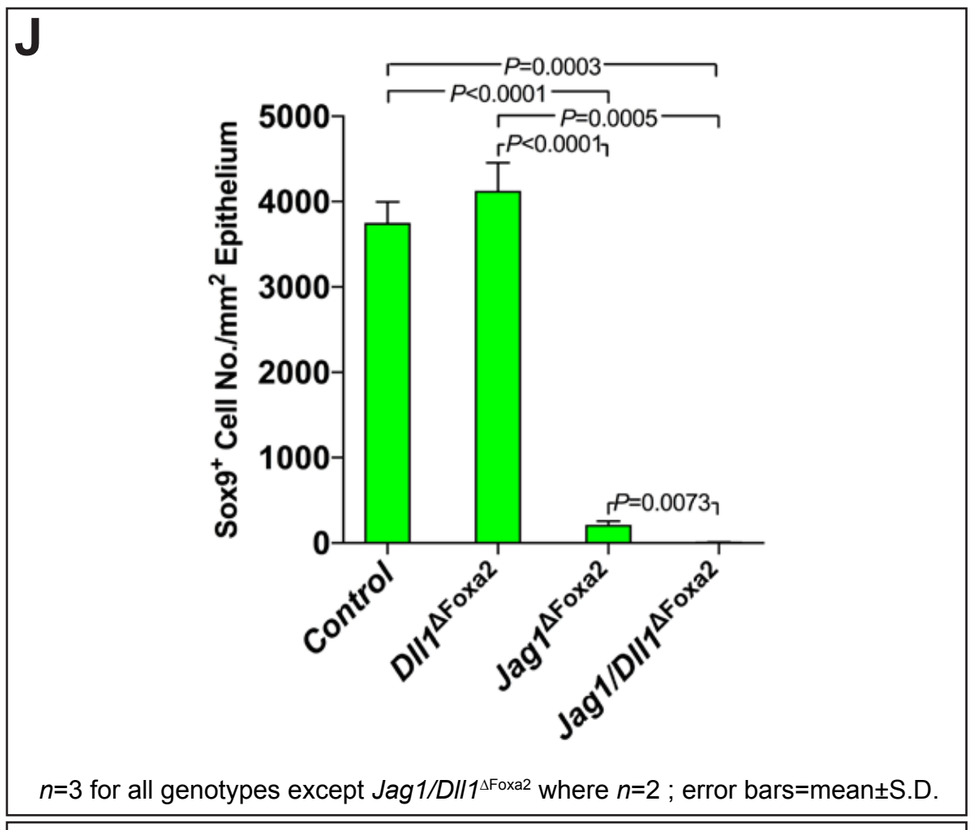

n=3 for all genotypes except *Jag1/Dll1*$^{\Delta Foxa2}$ where *n*=2 ; error bars=mean±S.D.

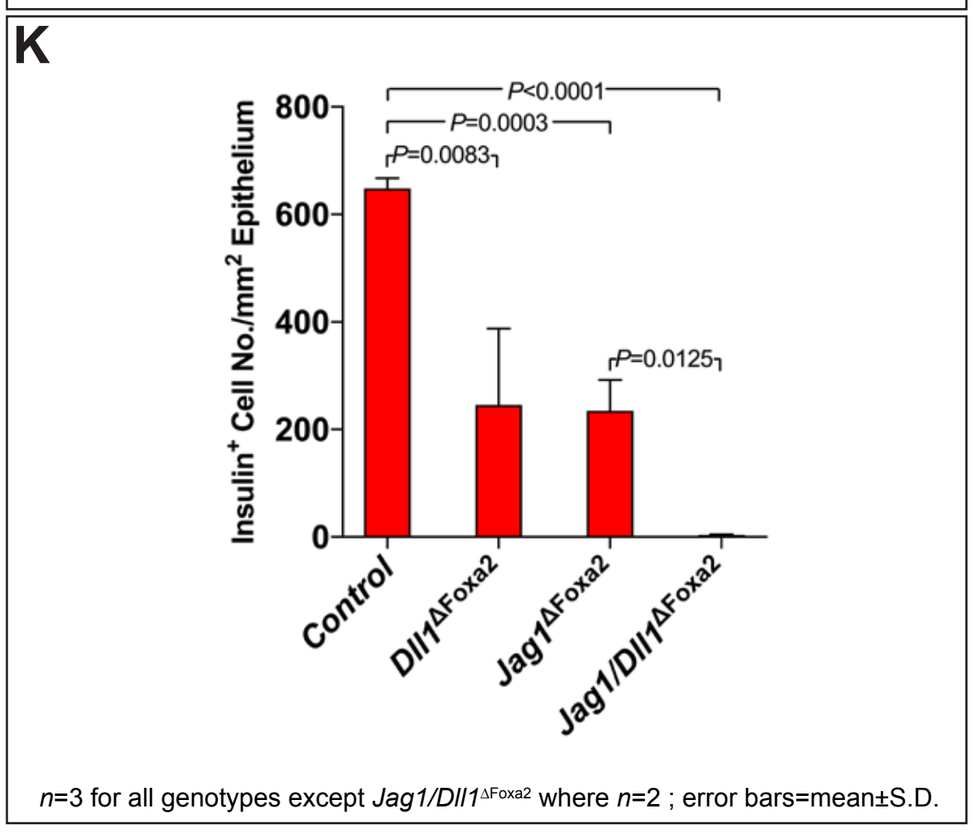

n=3 for all genotypes except *Jag1/Dll1*$^{\Delta Foxa2}$ where *n*=2 ; error bars=mean±S.D.